MASS SPECTROMETRIC STUDIES OF FISSION PRODUCTS FROM Pu^{239} AND U^{235}

MASS SPECTROMETRIC STUDIES OF FISSION PRODUCTS FROM Pu239 AND U235

By

HARRY ROBERT FICKEL, B.Sc.

A Thesis

Submitted to the Faculty of Graduate Studies

in Partial Fulfilment of the Requirements

for the Degree

Doctor of Philosophy

McMaster University

May 1959

DOCTOR OF PHILOSOPHY (1959)
(Chemistry)

McMASTER UNIVERSITY
Hamilton, Ontario

TITLE: Mass Spectrometric Studies of Fission Products From Pu^{239} and U^{235}

AUTHOR: Harry Robert Fickel B.Sc. (Queen's University)

SUPERVISOR: Dr. R. H. Tomlinson

NUMBER OF PAGES: XI, 116

SCOPE AND CONTENTS: The absolute cumulative yields of forty-one light and heavy fragments formed in the thermal neutron fission of Pu^{239} have been measured with a mass spectrometer using the isotope dilution technique. These include the yields of isotopes of rubidium, strontium, zirconium, molybdenum, ruthenium, cesium, cerium, neodymium and samarium. The yields of twelve light fragments formed in the thermal neutron fission of U^{235} have also been reported.

A comprehensive study of fission yields requires a knowledge of carrier-free separation techniques, accurate half-lives and neutron capture cross sections of the various fission nuclides. New procedures for the carrier-free analysis of the elements of zirconium, molybdenum and ruthenium have been developed. Also the half-lives of Sr^{89} and Zr^{95} and the thermal neutron capture cross sections of Xe^{135} and Sm^{149} were determined.

A comparison of the yields of the light and heavy mass fission products of Pu^{239} has made possible a more detailed understanding of neutron emission from the primary fragments of fission.

ACKNOWLEDGEMENTS

The author wishes to express his sincere gratitude and appreciation to Dr. R. H. Tomlinson to whom he is deeply indebted for his invaluable interest and guidance throughout the course of this work.

The completion of this work was made possible through the services extended by the Atomic Energy of Canada in the preparation and irradiation of the necessary plutonium and uranium sample and also by the financial assistance awarded by Canadian Industries Limited, International Nickel Company of Canada and McMaster University.

TABLE OF CONTENTS

	Page
GENERAL INTRODUCTION	1
HISTORICAL INTRODUCTION	4
(A) Determination of Absolute Yields of Nuclides in the Thermal Neutron Fission of Pu^{239}	4
(a) Radiochemical	4
(b) Mass Spectrometric	6
(B) Determination of Thermal Neutron Absorption Cross Sections	10
(a) Xenon-135	10
(b) Samarium-149	11
EXPERIMENTAL	11
(A) Mass Spectrometry	11
(a) Filament Assemblies	11
(b) Sample Loading	12
(c) Ionic Species	12
(d) Discrimination	13
(B) Carrier-Free Separation Techniques	14
(a) Zirconium	15
(b) Molybdenum	16
(c) Ruthenium	17
(C) Uranium-235	18
(a) Irradiation	20

TABLE OF CONTENTS (CONT'D)

	Page
(b) Chemical Procedures	20
(i) Treatment of Sample A	20
(ii) Treatment of Samples B and C	21
(iii) Treatment of Sample D	21
(D) Plutonium-239	21
(a) Preparation of PuO_2 samples	21
(b) Irradiation	22
(c) Chemical Procedures	24
(i) Treatment of Samples E and F	24
(ii) Treatment of Sample G	24
(iii) Treatment of Samples H and J	25
(iv) Treatment of Samples I and K	29
(v) Treatment of Sample L	29
(vi) Treatment of Sample M	32
(d) Standard Solutions for Isotope Dilutions	32
(i) Samples G and H	32
(ii) Barium for Sample H	33
(iii) Samples L and M	34
(iv) Molybdenum Solution	34
(v) Ruthenium Solution	35
(E) Neutron Flux and Effective Cross Section Determinations	35
Experimental Results	38
(A) Determination of Thermal Neutron Absorption Cross Section of Xe^{135}	38
(B) Determination of the Thermal Neutron Absorption Cross Section of Sm^{149}	41

TABLE OF CONTENTS (CONT'D)

	Page
(C) Determination of Half-Lives	43
(i) Strontium-89	43
(ii) Zirconium-91	43
(D) Relative Yields of Heavy Masses of Pu^{239}	43
(a) Cesium	43
(b) Samarium	47
(c) Neodymium	49
(d) Cerium	49
(E) Absolute Fission Yields of Ba^{136}, Cerium, Samarium Cesium and Neodymium Isotopes	51
(F) Relative Yields of Light Masses of Pu^{239}	61
(a) Rubidium	61
(b) Strontium	63
(c) Zirconium	63
(d) Yttrium	67
(e) Molybdenum	67
(f) Ruthenium	69
(G) Absolute Fission Yields of Rubidium, Strontium, Zirconium, Molybdenum and Ruthenium Isotopes ...	69
(H) Relative Yields in Thermal Neutron Fission of U^{235}	73
(a) Strontium	73
(b) Yttrium	80
(c) Neodymium	80
(d) Zirconium	80
(e) Molybdenum	84
(I) The Absolute Yields of the Light Mass Fragments in the Thermal Neutron Fission of U^{235}	84

TABLE OF CONTENTS (CONT'D)

Page

DISCUSSION

(A) Thermal Neutron Absorption Cross Section 87

(a) Xenon-135 89

(b) Samarium-149 90

(B) Relative and Absolute Yields of the Heavy Mass Fragments in the Thermal Neutron Fission of Pu^{239} . 92

(C) Relative and Absolute Yields of the Light Mass Fragments in the Thermal Neutron Fission of Pu^{239} and U^{235} 95

(D) Interpretation of the Fission Yields of Fragments Formed in the Thermal Neutron Fission of Pu^{239} and U^{235} 96

BIBLIOGRAPHY 104

APPENDIX 106

LIST OF TABLES

		Page
I	Absolute Yields in Thermal Neutron Fission of Pu^{239} Obtained from Literature	8
II	Irradiation Data For Uranium Samples	9
III	Irradiation Data For Plutonium Samples	23
IV	Standard Solution For Isotope Dilution of Sample G	26
V	Standard Solution For Isotope Dilution of Sample H	27
VI	On the Isotope Dilution of the Standard Solution of Barium Enriched in Ba^{134}	28
VII	Standard Solution For Isotope Dilution of Samples L and N	30
VIII	Isotope Dilution of Mo^{96} Enriched Solution	31
IX	Neutron Absorption Rates in Xe^{135}	36
X	Cobalt Monitor Data	39
XI	Effective Neutron Absorption Cross Section of Xe^{135}	40
XII	The Effective Neutron Absorption Cross Section of Sm^{149}	42
XIII	Mass Spectrometric Ratios of $\frac{Sr^{89}}{Sr^{90}}$	44
XIV	Measured Mass Spectrometric Ratios of $\frac{Zr^{95}}{Zr^{96}}$	45
XV	Relative Yields of Cesium Isotopes Produced in the Thermal Neutron Fission of Pu^{239}	46
XVI	Irradiation Times and Ratios of $\frac{Cs^{135}}{Y^{135}}$	110
XVII	Relative Yields of Samarium Isotopes Produced in the Thermal Neutron Fission of Pu^{239}	48
XVIII	Relative Yields of the Neodymium Isotopes in the Thermal Neutron Fission of Pu^{239}	50
XIX	Relative Yields of the Cerium Isotopes in the Thermal Neutron Fission of Pu^{239}	52

LIST OF TABLES

		Page
I	Absolute Yields in Thermal Neutron Fission of Pu^{239} Obtained from Literature	8
II	Irradiation Data For Uranium Samples	9
III	Irradiation Data For Plutonium Samples	23
IV	Standard Solution For Isotope Dilution of Sample G	26
V	Standard Solution For Isotope Dilution of Sample H	27
VI	On the Isotope Dilution of the Standard Solution of Barium Enriched in Ba^{134}	28
VII	Standard Solution For Isotope Dilution of Samples L and M	30
VIII	Isotope Dilution of Mo^{96} Enriched Solution	31
IX	Neutron Absorption Rates in Xe^{135}	36
X	Cobalt Monitor Data	39
XI	Effective Neutron Absorption Cross Section of Xe^{135}	40
XII	The Effective Neutron Absorption Cross Section of Sm^{149} .	42
XIII	Mass Spectrometric Ratios of $\frac{Sr^{89}}{Sr^{90}}$	44
XIV	Measured Mass Spectrometric Ratios of $\frac{Zr^{95}}{Zr^{96}}$	45
XV	Relative Yields of Cesium Isotopes Produced in the Thermal Neutron Fission of Pu^{239}	46
XVI	Irradiation Times and Ratios of $\frac{Cs^{135}}{Y^{135}}$	110
XVII	Relative Yields of Samarium Isotopes Produced in the Thermal Neutron Fission of Pu^{239}	48
XVIII	Relative Yields of the Neodymium Isotopes in the Thermal Neutron Fission of Pu^{239}	50
XIX	Relative Yields of the Cerium Isotopes in the Thermal Neutron Fission of Pu^{239}	52

		Page
XX	Mass Spectrometric and Isotope Dilution Data For Ce^{142} Produced in the Thermal Neutron Fission of Pu^{239}	53
XXI	Mass Spectrometric and Isotope Dilution Data for Nd^{149} Produced in the Thermal Neutron Fission of Pu^{239}	54
XXII	Mass Spectrometric and Isotope Dilution Data for Cs^{133} Produced in the Thermal Neutron Fission of Pu^{239}	55
XXIII	Mass Spectrometric and Isotope Dilution Data for Nd^{143} Produced in the Thermal Neutron Fission of Pu^{239}	56
XXIV	Mass Spectrometric Isotope Dilution Data for Ba^{138} Produced in the Thermal Neutron Fission of Pu^{239}	57
XXV	Cumulative Yields Based on the Calculated Number of Fissions	60
XXVI	Number of Fissions in the Plutonium Samples	62
XXVII	Cumulative Yields of the Heavy Mass Fragments Formed in the Fission of Pu^{239} together with Literature Values ...	64
XXVIII	Relative Yields of the Strontium Isotopes in the Thermal Neutron Fission of Pu^{239}	66
XXIX	Relative Yields of the Zirconium Isotopes in the Thermal Neutron Fission of Pu^{239}	66a
XXX	Relative Yields of the Yttrium Isotopes in the Thermal Neutron Fission of Pu^{239}	68
XXXI	Relative Yields of the Molybdenum in the Thermal Neutron Fission of Pu^{239}	70
XXXII	Relative Yields of the Ruthenium Isotopes in the Thermal Neutron Fission of Pu^{239}	71
XXXIII	Relative Yields of Isotopes of Various Light Fragments in the Thermal Neutron Fission of Pu^{239}	72
XXXIV	Mass Spectrometric and Isotopic Dilution Data for Rb^{87} Produced in the Thermal Neutron Fission of Pu^{239}	74
XXXV	Mass Spectrometric and Isotope Dilution Data for Cs^{133} in the Thermal Neutron Fission of Pu^{239}	75
XXXVI	Mass Spectrometric and Isotope Dilution Data for Sr^{90} Produced in the Thermal Neutron Fission of Pu^{239}	76

		Page
XXXVII	Mass Spectrometric and Isotope Dilution Data for Mo^{98} Produced in the Thermal Neutron Fission of Pu^{239}	77
XXXVIII	Mass Spectrometric and Isotope Dilution Data for Ru^{101} Produced in the Thermal Neutron Fission of Pu^{239}	78
XXXIX	Cumulative Fission Yields Normalized to the Ce^{133} Yield at 6.90%	79
XL	Relative Yields of the Strontium Isotopes in the Thermal Neutron Fission of U^{235}	81
XLI	Relative Yields of the Yttrium Isotopes in the Thermal Neutron Fission of U^{235}	82
XLII	Relative Yields of the Neodymium Isotopes in the Thermal Neutron Fission of U^{235}	83
XLIII	Relative Yields of the Zirconium Isotopes in the Thermal Neutron Fission of U^{235}	85
XLIV	Relative Yields of the Molybdenum Isotopes in the Thermal Neutron Fission of U^{235}	86
XLV	Relative Yields of the Measured Nuclides together with Literature Values	87
XLVI	Absolute Yields of the Light Fragments in the Thermal Neutron Fission of U^{235}	88
XLVII	Effective Absorption Cross Sections of Xe^{135} Calculated from Total Cross Sections	91

LIST OF ILLUSTRATIONS

		Page
Figure 1.	$\frac{Sr^{89}}{Sr^{90}}$ vs. time	112
Figure 2.	$\frac{Zr^{95}}{Zr^{96}}$ vs. time	113
Figure 3.	Mass Yields in Thermal Neutron Fission of Pu^{239}	114
Figure 4.	Comparison of the Light and Heavy Mass Yields in the Thermal Neutron Fission of Pu^{239}	115
Figure 5.	Comparison of the Light and Heavy Mass Yields in the Thermal Neutron Fission of U^{235}	116
Figure 6.	Comparison of Light Mass Yields in Thermal Neutron Fission of Pu^{239} and U^{235}	117
Figure 7.	Comparison of Heavy Mass Yields in Thermal Neutron Fission of Pu^{239} and U^{235}	118

General Introduction

The bombardment of heavy nuclei with neutrons possessing energy above a certain lower limit causes fission to occur. The neutron entering the nucleus produces a highly excited state due to its binding energy. The nucleus then splits into two fragments which separate with considerable kinetic energy. De-excitation of these fragments (which are neutron-rich) occurs either by the emission of neutrons followed by β^- decay or simply by β^- decay until nuclear stability is attained. The series of nuclides through which the fragment passes by β^- decay is referred to as the "chain" of the particular mass.

The primary fission yield of a nuclide is the percentage of fissions which results in the formation of that particular nuclide. The sum of all the primary yields of a particular mass chain is known as its cumulative fission yield.

In fission induced by thermal (slow) neutrons, a characteristic "double-humped" curve is obtained when cumulative fission yield is plotted against mass. From this, it is apparent that in the fission process the excited nucleus favours a division into two fragments of unequal mass rather than two fragments of equal mass. Although this was known within a few months of the discovery of fission, no detailed theory has yet explained this observation.

A detailed knowledge of the yields of each of the nuclides as well as their half-lives and neutron absorption cross sections obtained in

fission is valuable in reactor design. Such factors determine the length of time the fuel may be used effectively. The information also assists in the formation of theories on nuclear structure, and, will inevitably aid in the formulation of a theory for nuclear fission.

The absolute fission yields of many nuclides formed by the bombardment of U^{235} by thermal neutrons have already been determined. However, the values for the absolute yields of fission nuclides from Pu^{239} are not as well established. The yields determined by radiochemical methods have been summarized by Steinberg et al. (1), (2). Their summation, including values interpolated from a smooth mass-yield curve, total only 87.61% and 93% respectively for the heavy mass fragments. This indicates considerable error in either the measured or interpolated values. Mass spectrometric values for the absolute yields of the heavy fragments were published by Wiles et al. (3) and later by Krishanski et al. (4). In the work of Wiles et al. (3) only 80% of the fission products was recovered in the procedure of dissolving the irradiated PuO_2. It was pointed out in their discussion that the yields reported would be inaccurate if the losses of the various elements were not equal. The yields obtained by Krishanski et al. (4), although in essential agreement with those of Wiles, are not independent since only relative yields were actually measured and these normalized to Wiles' absolute yield values.

This thesis reports on the determination of the relative and absolute yields of 41 mass chains formed in the thermal neutron fission of Pu^{239} and 12 yields of U^{235} fission products. The study of yields of fission products also necessitates the knowledge of accurate values for neutron absorption cross section and the half-lives of unstable nuclides.

The cross section of Xe^{135} is of great interest not only in fission yield determinations but also in reactor operations since it is formed in a relatively high yield and possesses an abnormally high thermal neutron absorption cross section. The values of the total cross section of Xe^{135} reported in the literature differ by about 10% and hence its redetermination is of interest. In the present work, an attempt has been made to evaluate the neutron absorption cross section by a comparison of the mass spectrometric ratios of Cs^{135}/Cs^{137} obtained at high and low neutron fluxes. The value estimated is in agreement with the value reported by Bernstein. The thermal neutron absorption cross section of Sm^{149} was also evaluated from the change in ratio of Sm^{150}/Sm^{149} found in irradiated natural samarium.

The half-lives of Sr^{89} and Zr^{95} were determined by observing the change in the ratio of fission product Sr^{89}/Sr^{90} and Zr^{95}/Zr^{96} as a function of time.

The relative yields of isotopes of cesium, cerium, neodymium and samarium were determined and their absolute yields estimated together with that of Ba^{138} with the mass spectrometer using the isotope dilution technique. Similarly, the absolute fission yields of the light mass products formed in thermal neutron fission of both Pu^{239} and U^{235} were determined.

The accurate determination of forty-one cumulative fission yields from Pu^{239} permits the determination of nuclide masses having corresponding yields. This comparison has made it possible to deduce the neutron emission from complementary fission fragments.

Historical Introduction

(A) Determination of Absolute Yields of Nuclides in the Thermal Fission of Pu^{239}.

(a) Radiochemical

Relative values of fission yields were first obtained for radioactive nuclides by radiochemical separations and counting techniques.

To obtain relative fission yields by radiochemical methods a sample of fissile material is irradiated with neutrons. After irradiation, known amounts of each of the various elements found in fission are added as carriers for the fission products. These are chemically separated from each other and the counting rate obtained in each element. From the chemical recovery of the added carrier, the half-life of the radioisotope counted, and the time of irradiation and analysis, it is possible to evaluate the number of atoms of each of the various radionuclides produced. Such procedures are described in detail by Coryell and Sugarman[5]. However, without this knowledge for all the nuclides, the absolute values could be determined only by knowing the total number of fissions which had occurred in the irradiated material. D. W. Engelkemeir et al. [6] and H. S. Freedman et al. [7] have used one of the more refined procedures for measuring the total number of fissions occurring during an irradiation.

They have used a fission chamber consisting of a thin film of the fissile material of known mass placed on a 1 mil. platinum foil in a pulse

ionization chamber filled with argon (8). This chamber and a larger sample of the fissile material were irradiated in a position of constant neutron flux in a reactor. The number of fissions occurring in the large sample was calculated from the total number of fissions counted in the pulse ionization chamber and the relative weights of the samples.

E. P. Steinberg's summary of absolute fission yields (1) based on weighted averages of relative and absolute yields reported previous to 1951 are shown in column 2, Table I. Revised values published by Steinberg in 1955 (2) are tabulated in column 3, Table I.

Absolute-yield experiments led to values of 5.93% for 67 hr Mo^{99} and 4.90% for 12.8 d Ba^{140}. These two nuclides were then used as reference standards for converting relative yields of other nuclides into absolute values. Many improvements in counting techniques have occurred since the earliest fission yield data were reported. Using data from papers reporting the effects of sample weight and backing material on counting rate (9), (10) Steinberg recalculated a value of 5.36% for the fission yield of 12.8 d Ba^{140}. The increased value for the reference standard has been applied in determining the revised values shown in column 3, Table I.

Steinberg and Freedman estimate an accuracy of 10% and a precision of 5% for the values in column 3, Table I. The limited number of yields which had been determined restricted the form of the yield % vs. mass relationship to a smooth double-humped curve. Recent improvements in counting techniques such as those reported by Yaffe (11), (12) now make it possible to obtain more accurate values for fission yields by radiochemical methods, but these have not yet been applied to fission yield studies with Pu^{239}.

(b) Mass Spectrometry

The advent of mass spectrometry into the field of fission yield determinations has increased the number of nuclides which have been studied. This has occurred mostly for mass chains having only short-lived radionuclides which may be difficult to isolate for counting, but may be measured from the stable end products with the mass spectrometer.

Also it was possible to obtain 1-2% precision for the relative yield determinations for the isotopes of an element. The actual number of atoms of each isotope of the nuclides can be estimated by an isotope dilution technique to give absolute accuracy of about 3% to each fission yield (13).

This involves the determination of the ratio of the yields of two isotopes of an element and then a redetermination of this ratio after the addition of a known number of atoms of the element with a markedly different isotopic abundance. The number of atoms of the fission isotopes can then be calculated since there are two equations and only two unknown quantities.

The absolute fission yield of a particular nuclide may then be estimated by dividing the number of atoms of it determined by isotope dilution by the number of fissions (13), (14).

The number of fissions occurring in the irradiated material may be obtained by various methods such as the determination of the depletion of the fissile material (15), the direct measurement using a fission counter (8), or indirectly from a flux monitor (14), (16). The determination of the depletion of the fissile material can be achieved with large samples by separation and weighing of the remaining fissile

material after the irradiation, or with smaller samples by measuring the change in the ratio of the fissionable isotope to a non-fissionable isotope. However, in both instances, at least 10-50% depletion is required which necessitates the handling of materials with high specific activities.

The use of a fission counter in a reactor is limited by its size. Also, the flux may differ considerably between the material in the counter and the sample which is to be analyzed since these are physically separated.

B^{10} possesses a thermal neutron absorption cross section of 4037 barns compared to the fission cross section of 582 ± 2 barns for U^{235} and 746 ± 8 barns for Pu^{239}. Since the (n, α) cross section of B^{10} is much larger than the fission cross sections of either U^{235} or Pu^{239}, there will be a much greater loss in the B^{10} of the monitor than in these fissile materials during a particular irradiation. The number of fissions may be calculated from the change in the measured B^{10}/B^{11} ratio using the known ratio of the neutron fission cross section of the fissile material to the neutron absorption cross section of B^{10}.

Cobalt is anisotopic in nature occurring as Co^{59}. The thermal neutron capture cross section of Co^{59} is considerably lower than the fission cross sections of the fissile materials. Therefore the amount of Co^{60} formed in a cobalt monitor which is simultaneously irradiated with a sample of fissile material is many times less than the amount of fission products. However, it can be accurately determined by taking

TABLE I

Absolute Yields in Thermal Neutron Fission of Pu^{239}

Obtained from Literature

Fission Product	Yield Percent			
	Steinberg et al. (1)	Steinberg et al. (2)	Wiles et al. (3)	Katcoff (17)
49-h Zn^{72}	0.00011	0.00011		0.00012
2.4-h Ru^{103}	0.073	0.080		0.085
51-d Sr^{89}	1.8	1.8		1.9
9.7-h Sr^{91}	2.1	2.3		2.4
58-d Y^{91}	2.9	2.8		3.0
65-d Zr^{95}	5.6	5.6		5.9
17-h Zr^{97}	5.2	5.5		5.6
66-h Mo^{99}	5.9	6.1		5.9
39.7-d Ru^{103}	5.6	5.5		5.8
35.3-h Ru^{105}	3.8	3.7		3.9
1.01-y Ru^{106}	3.8	4.7		5.0
13.4-h Pd^{109}	1.0	1.0		1.5
7.6-d Ag^{111}	0.25	0.27		0.27
21-h Pd^{112}	0.10	0.10		0.10
43-d Cd^{115m}	0.003	0.003		0.003
53-h Cd^{115}	0.045	0.045		0.038
Total 115		0.048		0.041
27.5-h Sn^{121}		0.041		0.044
9.6-d Sn^{125}		0.068		0.072
91-h Sb^{127}	0.37	0.37		0.39

TABLE I (Continued)

Fission Product	Yield Percent			
	Steinberg et al. (1)	Steinberg et al. (2)	Wiles et al. (3)	Katcoff (17)
8.05-d I^{131}	3.6	3.6		3.8
Stable Xe^{131}			2.71	2.87
77-h Te^{132}	4.9	4.9		5.2
Stable Xe^{132}			3.79	4.02
20.8-h I^{133}	5.0	5.0		5.3
5.27-d Xe^{133}			4.97	5.27
Stable Cs^{133}			4.97	5.27
Stable Xe^{134}			5.37	5.69
6.7-h I^{135}	5.3	5.5		5.8
2.6×10^6-y Cs^{135}		1.9	5.22	5.53
86-s I^{136}				2.1
Stable Xe^{136}			4.77	5.06
29-y Cs^{137}		5.8	4.94	5.24
84-m Ba^{139}	5.2	5.4	6.61	5.7
12.8-d Ba^{140}	4.9	5.36	7.36	5.68
Stable Ce^{140}			7.36	5.68
33-d Ce^{141}	4.4	4.9	6.94	5.2
Stable Ce^{142}			6.62	6.69
33-h Ce^{143}	4.3	5.1		5.4
Stable Nd^{143}			5.98	6.31
285-d Ce^{144}		3.7	5.00	5.29
Stable Nd^{144}			5.00	5.29

TABLE I (Continued)

Fission Product	Yield Percent			
	Steinberg et al. (1)	Steinberg et al. (2)	Wiles et al. (3)	Katcoff (17)
Stable Nd^{145}			4.07	4.24
Stable Nd^{146}			3.36	3.53
Stable Sm^{147}			2.81	2.92
Stable Nd^{148}			2.27	2.28
Stable Sm^{149}			1.81	1.89
Stable Nd^{150}			1.31	1.38
80-y Sm^{151}			1.10	1.17
Stable Sm^{152}			0.88	0.85
47-h Sm^{153}		0.39	0.64	0.41
Stable Sm^{154}			0.40	0.32
24-m Sm^{155}			0.30	0.22
15.4-d Eu^{156}		0.12		0.12

advantage of its radioactive character. As in the case of the boron, the number of fissions may be determined from the extent of neutron capture in the Co^{59} using the known ratio of the neutron fission cross section of the fissile material to the neutron capture cross section of the Co^{59}.

D. M. Miles et al (3) determined the absolute fission yields of the heavy fission fragments of Pu^{239} using a mass spectrometer. The relative isotope abundances of cerium - 140, 142 and 144 were normalized to the absolute yields of the neodymium isotopes through the 144 mass chain. Since Ce^{144} has a half-life of 278 days, the yield of the 144 mass chain may be compared to those of the 140 and 142 mass chains through the cerium isotope ratios in young fission products. In old fission products where the Ce^{144} has decayed through Pr^{144} to Nd^{144}, the yield of the 144 mass chain may be related to those of the 143, 145, 146, 148 and 150 mass chains through the absolute yields of the neodymium isotopes obtained by isotope dilution.

After interpolation of the unmeasured yields, Miles et al. (3) normalized the values to total 100%. The values obtained are shown in column 4, Table I.

L. M. Krishansky et al. (4) have published absolute yields for various mass nuclides. Relative yields were measured with a mass spectrometer and normalized to Miles' data at Cs^{137} and Nd^{143}. These values are essentially the same as those tabulated in column 4, Table I.

S. Katcoff (17) has prepared the most recent summary of absolute fission yields by weighting all the available data. This compilation for Pu^{239} is shown in column 5, Table I. Greater value was placed on mass

spectrometric determinations because of their greater accuracy. It should be noted that in this summary, Katcoff has normalized both the light and heavy mass yields to 100% and in so doing increased the absolute yield of Ba^{140} and other nuclides reported by Steinberg et al. (2) by 6%.

Simultaneous with the work in this thesis, the absolute yields of some nuclides of xenon and krypton formed in the thermal neutron fission of Pu^{239} were measured by K. Fritze et al. (16). These values will be considered in greater detail in the discussion.

(B) Determination of Thermal Neutron Absorption Cross Sections

(a) Xenon-135

Measurements of the total cross section of Xe^{135} have been made at Oak Ridge National Laboratories by E. Bernstein (18) using a crystal spectrometer, and by E. G. Smith (19) using a fast chopper. Differences of about 10% exist in the results of the two methods, and at present there is no basis for favouring either one or the other's data. Westcott (20) has tabulated both sets of data along with calculated values of the effective absorption cross section. The values depend on the choice between possible values of $g = 5/8$ and $g = 3/8$ for the statistical weight factor and hence the total cross section measurements leave considerable uncertainty in the value of the effective absorption cross section.

The effective neutron cross section has been measured by Petruska et al. (14) and Ivanov et al. (21) using mass spectrometric techniques. Since Cs^{135} is the daughter of the short-lived Xe^{135} nuclide, it is possible to evaluate the neutron absorption cross section of Xe^{135} by

comparison of the ratios of Cs^{135}/Cs^{137} from fission product samples obtained at high and low neutron fluxes. Values of the neutron temperature were not determined for either of the effective neutron absorption cross section measurements made by Petrusha et al. (14) or Ivanov et al. (21) and hence comparison of them either with each other or with the total cross section values is not possible.

(b) Samarium-149

The effective neutron absorption cross section of Sm^{149} is strongly dependent on the neutron energy distribution. In view of the sensitivity to the neutron temperature it is not surprising that values varying from 47,000 barns (22) to 74,500 barns (23) have been reported in the literature. Assuming the variation in total cross section with neutron energy given by Hughes (24), Westcott (20) has calculated the effective thermal neutron absorption cross section for various temperatures based on the accepted value of 37,700 barns for the 2200m/sec. cross section.

EXPERIMENTAL

(A) Mass Spectrometry

All the fission product analyses reported in this thesis were performed using the ten-inch radius, 90-degree-sector, solid source mass spectrometer equipped with magnetic scanning and a ten-stage electron multiplier described by D. Irish (25).

(a) Filament Assemblies

Several of the initial analyses of strontium, yttrium and zirconium were performed using a single tungsten filament, 0.001 inches

thick and 0.030 inches in width which had been coated with platinum. Platinum has a higher work function than tungsten hence a higher ionization efficiency. The use of a platinum ribbon filament is restricted by the lower melting point of platinum.

The tungsten filament was electrically heated in vacuo to approximately 2000°C for 45 minutes to clean the surface. Platinum was electrolytically deposited in a black irregular form from a 1% solution of chloroplatinic acid. A smooth metallic surface was obtained by re-heating the filament in vacuo to 2000°C for 45 minutes.

However, later analyses showed that higher ion efficiencies could be produced in a multiple filament source (26), by evaporation from a relatively cool sample filament to a hot filament where the ions are produced.

(b) Sample Loading

Using a single platinized filament, a small drop of the concentrated solution to be analyzed was added to the filament and evaporated to dryness. Low currents were used in the heating to avoid loss of sample due to evaporation or spattering (i.e. 1-2 amps).

The tungsten filaments for the multiple filament source assembly were cleaned by heating in an evacuated system or in the mass spectrometer for 10-12 hrs. at currents of 5 amps. A drop of the solution was placed on the sample filament and evaporated as described for the single platinized filament.

(c) Ionic Species

With the exception of yttrium and zirconium, the ionic species and the relative filament currents at which they appear with a single

platinized tungsten filament have been discussed in a previous thesis (27).

Yttrium appears as the oxide ion (YO^+) at a filament current slightly higher than that required for the Sr^+ ion. Zirconium appears both as the metal Zr^+ ion and as the oxide ZrO^+, the latter oxide species being more abundant.

Using a multiple filament source, the order of appearance of the elements remains the same, however, the sample filament current is considerably less, and in fact, the Cs^+ and Rb^+ ions appear with ion filament currents of 3.5-4.0 amps even without current flowing through the sample filament. By proper adjustment of the filament currents, the CeO^+ peaks can be obtained free from interfering NdO^+, and similarly, neodymium ion currents can be measured with a minimum cerium correction. Molybdenum and ruthenium form the metal ions Mo^+ and Ru^+ respectively at relatively high filament currents.

(d) Mass Discrimination

Mass discrimination in the mass spectrometer due to non-linearity of the multiplier with mass has been discussed by D. Irish (25). The value for the relative abundances of the neodymium isotopes were constant within the 1% precision possible with the mass spectrometer whether the collection of ions was obtained with or without the multiplier. Thus, it was concluded that no significant mass discrimination was caused by the multiplier.

However, the measured ion currents obtained with the mass spectrometer for the isotopes present in natural neodymium differed

systematically from the published relative abundances. The systematic error indicated a non-linearity in the Applied Physics Corporation vibrating reed electrometer and/or the Leeds and Northrup Speedomax recorder. The voltages required to duplicate those obtained from the electron multiplier during an analysis were measured with a potentiometer. Provided the electron multiplier has no mass discrimination these voltages are directly proportional to the ion currents and hence non-linearity in the electrometer and recorder are eliminated. The values for the abundances of the neodymium isotopes obtained from these relative voltages were in agreement with the published values.

The determination of the voltages required to duplicate ion currents also allowed a comparison of ion currents differing by 100 fold or more.

(5) Carrier-Free Separations

The quantities of fission product in the samples analyzed were usually quite small and hence efficient chemical separations were required in order to provide sufficient quantities for mass spectrometric analysis.

In radiochemical analysis a quantitative fraction of the radioactive isotope being studied must be recovered from the irradiated sample. A relatively large quantity of the stable isotopes of the element can be tolerated in counting the radioactive isotope provided suitable corrections are made for the self-absorption and backscatter of the radiation. An increase in the quantity of added element increases the accuracy of the quantitative determination, but also increases the counting corrections.

However, when an attempt is made to minimize the self-absorption in the sample by the addition of smaller quantities of the carrier, the

accuracy of the quantitative determination of the chemical recovery of the carrier is also decreased.

The increased efficiency of the separation on addition of the carrier may be illustrated by a precipitation in which the Ksp of the precipitating compound requires 90% of the radioactive isotope present to remain in solution and hence 10% recovery has been achieved. However, if stable isotopes of the element are added to the solution in the ratio of 99:1 only 0.01 of the element remaining in solution will be the radioactive isotope. The efficiency of the radioactive isotope recovery has been increased to 99.1%.

In mass spectrometric analysis, only isotopic ratios are measured and therefore quantitative chemical separations are not required. Only a representative sample having the same isotopic abundances as the original sample must be obtained. Thus, carriers can not be used in the separations. Contamination of the sample with the natural occurring element must be avoided. When the natural element includes one or more isotopes which are not present in the sample being analyzed, appropriate corrections may be applied for contamination, however, when the same isotopes appear in both the natural element and the sample, no correction is possible.

(a) Zirconium

Uranium may be separated from most fission products by precipitating from a neutral solution using H_2O_2. Zirconium under these conditions forms a colloid which is carried down with the precipitate. However, advantage can be taken of this colloidal-forming tendency to achieve a carrier-free separation of zirconium from most of the other fission elements and the uranium itself.

When a neutral solution of an irradiated sample is dialyzed the colloidal zirconium is isolated from the uranium and most of the other fission products.

The simplicity of the procedure makes this a very attractive method, but the presence of certain anions in the solution increases the quantity of zirconium which dialyses (28). For maximum efficiency the solution should have a pH greater than 5 and be completely free from such anions as F^-, $C_2O_4^=$ and $PO_4^{\equiv}$.

A solution of the irradiated material containing fission product zirconium was evaporated to dryness and redissolved in water twice to remove excess acid. The final volume of 0.75 ml was pipetted into a dialyzer. The solution was dialyzed three times for 12 hr. period using 250 ml of water each time. The contents of the dialyzer was then pipetted into a Vycor crucible. Approximately half of the zirconium remained in the dialyzer, but this was recovered by washing with 0.5 ml of HNO_3. The solution in the crucible, along with the washings, was then evaporated to approximately 0.25 ml for use in the mass spectrometer.

(b) Molybdenum

Molybdenum may be extracted from an aqueous solution using various organic reagents (29). One of the most efficient methods is the extraction from an aqueous 6N HCl solution employing ethyl ether saturated with 6N HCl. The molybdenum is separable from the fissile material and most of the remaining fission products. However, in attempting a separation from uranium, the solution must be free from nitrate ions (NO_3^-) since uranyl nitrate is also extractable under these conditions.

In most samples studied, the dialysate from the zirconium

separation was used for isolation of the molybdenum. This solution was evaporated to 5 ml and after the addition of 1 ml of freshly distilled HCl taken to dryness in a centrifuge tube using a heat lamp. This was repeated three times to ensure the removal of nitrate. The sample was dissolved in 2 ml of water and evaporated to dryness twice to remove excess acid. The final solid was dissolved in approximately 1.5 ml of 6N HCl and extracted three times with 1.5 volumes of ethyl ether saturated with 6N HCl. These extractions were carried out in the centrifuge tube, the ether layer being removed with a 2 ml syringe. The ether fractions were combined and concentrated to 0.5 ml. This solution was used for the mass spectrometric analysis.

(c) Ruthenium

Ruthenium can be separated from other elements by means of an oxidative distillation. When oxidized in an acid solution, ruthenium forms volatile ruthenium tetroxide which can be distilled and collected in an aqueous solution containing an appropriate reducing agent.

Since only small amounts of reducing agent were used in the receiver, the ultimate concentration of the distillate could lead to the subsequent loss of ruthenium if the oxidant also distilled. Therefore a potassium permanganate-sulphuric acid oxidative solution (30) was used in preference to $HClO_4$ which has been used by many other workers (31).

The distillation was carried out in a glass apparatus. A solution of the irradiated material in about 4.5 ml was placed in a distillation flask along with 3 ml of 0.16N $KMnO_4$ and 7.5 ml of 36N H_2SO_4.

The distillate from the flask which was obtained on heating was carried to a series of three traps by means of a slow stream of air. The

first trap contained water with a few drops of H_2O_2 and HNO_3 added to reduce the ruthenium tetroxide. This trap was cooled in an ice bath. The second and third traps contained concentrated HCl to absorb any escaping tetroxide.

A pulse height analyzer was used to check the distillate fractions for Rhodium 106, which is the short-lived daughter of 1.01 yr. Ru^{106} and emits γ-rays of energy 0.51 Mev. and 0.62 Mev. Most of the ruthenium was found in the first trap. This solution after evaporation to a volume of about 0.25 ml was used for mass spectrometric analysis.

(C) Uranium - 235 Samples

(a) Irradiation

Table II summarizes the irradiation data for all the uranium samples used in this report.

Sample A was a block of natural uranium and B was UO_2 in which the uranium was 7% enriched in U^{235}.

B and C were used for the determination of the thermal neutron absorption cross sections of Xe^{135} and Sm^{149}.

These were block assemblies having five equally spaced holes, prepared using super pure magnesium. In the central position was placed a quartz vial (0.10" diameter x 0.5" long) wrapped in aluminum containing 10 micrograms of samarium in solution. The pins of uranium-aluminum alloy (0.108 cm. diameter and 0.965 cm. in length containing 1 mg. U^{235}) crimped in super pure aluminum tubing were located in positions on either side of the samarium. Cobalt flux monitors (0.005" diameter and 1 cm. in length weighing approximately 1.15 mg.) sheathed in aluminum tubing were

TABLE II

Irradiation Data for Uranium Samples

Sample		Weight (g)	Irradiation Time (days)	Reactor Position	Average Neutron Flux x 10^{12} (n $cm^{-2}sec^{-1}$)
A		3.755	23.5	J Rod anulus	9.0*
B	Top	0.01	3.66	S - 6 - 3	3.102
	Bottom	0.01	3.66	S - 6 - 3	3.111
C	Top	0.01	3.66	S - 3 - 5	11.17
	Bottom	0.01	3.66	S - 3 - 5	11.63
D		0.205	195		2.4*

*Value is approximate, obtained from Reactor Operation Report.

Sample A was a block of natural uranium and D was UO_2 in which the uranium was 7% enriched in U^{235}.

placed in the outside positions. Two such assemblies were simultaneously installed at positions B-3-5 and B-6-3 in the graphite reflector of the NRX reactor, Chalk River, and irradiated for 87.33 hrs. without shut-downs or serious power fluctuations. This time at the flux of these positions was more than that required to ensure 2% precision in the measured values of the effective neutron absorption cross sections. During the irradiation the reactor power was constant within 0.5%, 8 hr. power checks showing random fluctuations about 40.4 megawatts, not exceeding 0.3 megawatts at any time.

(b) Chemical Procedures

(i) Treatment of Sample A

The dark dull surface of the metallic uranium sample was cleaned with dilute freshly distilled nitric acid producing the bright silvery lustre of metallic uranium. The washings which would contain any possible surface contamination were discarded. The metal was placed in a vycor crucible and dissolved in 2 ml of freshly distilled 12 N nitric acid, warming the solution from time to time by means of a heat lamp to aid in the dissolution. The resultant uranyl nitrate solution was evaporated to dryness in order to remove excess HNO_3. The remaining solid was dissolved in 10 ml of de-ionized distilled water and dialyzed for recovery of zirconium as discussed in section B (a). The dialysate was evaporated to dryness and re-dissolved in de-ionized distilled water. This was repeated several times to ensure the absence of free acid since uranium can not be quantitatively precipitated in an acid solution using H_2O_2. The uranium was then precipitated as $UO_4.2H_2O$ by the addition of 30% H_2O_2.

The mixture was centrifuged and the supernatant liquid which contained most of the fission products was decanted.

The solution was returned to the crucible, concentrated to approximately 0.25 ml and used for mass spectrometric determinations.

(ii) Treatment of Samples B and C

These samples were dissolved separately in vycor crucibles using HCl and HNO_3, the aluminum sheaths being dissolved with their particular pins, with the exception of the sheath from the top of sample C. Each solution was evaporated to dryness and the white solid dissolved in 10 ml of de-ionized distilled water. The aluminum was precipitated as $Al(OH)_3$ using NH_4OH and the supernatant liquid evaporated to dryness. The remaining solid was dissolved in aqua regia, the solution heated on a steam bath for 10-15 minutes and then evaporated to dryness. This was repeated several times to ensure the absence of NH_4^+ salts. The solid was finally dissolved in 0.25 ml of water. This solution was used for mass spectrometric analysis.

(iii) Treatment of Sample D

The irradiated sample was placed in distilled HNO_3 to clean the surface, after which it was transferred to a small beaker and dissolved in 2 ml of distilled HNO_3. Zirconium and molybdenum were isolated in the manner discussed in section B.

(D) Plutonium-239

(a) Preparation of PuO_2 samples

97 mg. of plutonium IV nitrate having composition of 97% Pu^{239} and

3% Pu^{240} were dissolved in a volume of 2 ml of 8M HNO_3.

A Dowex I resin column 10 cm long and 1 cm in diameter was conditioned by washing with 11M distilled HCl, then de-ionized distilled water and finally with more 11M HCl. The plutonium was absorbed on the on the column from its solution and washed with 11M, 8M and 6M HCl respectively, the washing solutions being discarded. The plutonium was finally eluted with 3M HCl.

The solution was evaporated to dryness in a vycor crucible using a heat lamp. The solid was dissolved in distilled conc. HNO_3 and the green plutonium nitrate solution evaporated to dryness. The crucible was then heated to a dull red heat for 15 minutes, using an open flame, to convert the plutonium nitrate into the greenish-yellow oxide (PuO_2). The conversion was carried out at a low temperature and for a short heating period since prolonged heating at high temperatures increases the insolubility of the resulting oxide.

Approximately 10 mg samples of PuO_2 were measured into fine quartz tubes and the tubes sealed by drawing off the quartz. The tubes were checked for leaks by dropping them into boiling water and watching for signs of bubbles.

(b) Irradiation Data for all Plutonium Samples are Summarized in Table III.

For samples used in absolute yield determinations, further information than that given in Table III is required. Sample C consisted of 0.01012 g. of PuO_2 in which 93.3% of the total plutonium was Pu^{239}. The oxide was contained in a quartz tube. The dimensions of the oxide in the tube were 0.545 cm radius and length 0.3 cm.

TABLE III

Irradiation Data for Plutonium Samples

Sample	Weight (g)	Chemical Form	Irradiation Time (days)	Average Neutron Flux x 10^{13} (n/cm^2/sec)
E	0.01091	PuO_2	31.2	0.56*
F	0.01034	PuO_2	31.03	1.00*
G	0.01012	PuO_2	31.57	0.346
H	0.0758	15.9% Pu-Al alloy	23.53	0.194
I	0.1520	15.9% Pu-Al alloy	34	0.86
J	0.1966	15.9% Pu-Al alloy	30.0	0.511
K	0.10551	10% Pu-Al alloy	30	6.6*
L	0.10061	10% Pu-Al alloy	34	5.56
M	0.10561	10% Pu-Al alloy	25	7.00

*Only approximate, obtained from Reactor Operation Report.

Sample E was a Pu-Al alloy disc 0.3125" in diameter and 0.0205" thick containing 13.9% plutonium of which 96.1% was Pu^{239}. Only half of the sample was used in the isotope dilution. This weighed 0.0410 g.

(c) Chemical Procedures

(i) Treatment of Samples E and F

Samples E and F were treated in the same manner. The irradiated material was transferred from its quartz tube to a platinum crucible which was fitted with a platinum cover. Approximately 1.5 ml of HF was added and the crucible warmed with a heat lamp. When the solution containing the undissolved portion of the PuO_2 had evaporated to a small volume, 4-5 drops of distilled HCl were added and the solution taken to dryness. This hot HF-HCl treatment was continued for two weeks until the sample was completely dissolved. The final solution which was yellow in colour was evaporated to dryness and the residue dissolved in 1-1.25 mls of de-ionized distilled water.

A small part of this solution was used directly for cesium, strontium and yttrium determinations and the remainder for zirconium and molybdenum with the procedures discussed in section B.

(ii) Treatment of Sample G

This PuO_2 sample was used in the determination of absolute fission yields by the isotope dilution technique, thus in the treatment of this sample, extreme care was taken against loss of fission products. The contents of the quartz tube was transferred to a platinum crucible. The tube was washed with HF until the beta activity remaining in the tube was negligible. The washings were added to the crucible. The hot HF-HCl

treatment was carried out in the same manner as described for samples E and F. The solution was then evaporated to dryness and the residue dissolved in 2 ml of 1N HCl.

Less than 0.01 ml of this solution was analyzed in the mass spectrometer for the isotopic ratio of the elements, strontium, cesium, neodymium and samarium. 0.24075 g. of the isotope dilution solution whose composition is given in Table IV was added to the remainder of the sample solution. This was accomplished by taking up approximately 0.25 ml in a polythene pipette and weighing the pipette before and after dispensing the solution.

After standing for 48 hrs. the solution was evaporated to dryness, then the residue re-dissolved in 1.5 ml of distilled HCl. This was repeated three times to equilibrate the fission products with the components of the isotope dilution solution. A portion of this solution was analyzed with the mass spectrometer for each of the elements that were isotope diluted. Molybdenum was separated from the remainder of this solution by the procedure already described in section B (b) and analyzed with the mass spectrometer.

(iii) Treatment of Samples H and J

Sample H was cut approximately in half. The weighed half which was to be used for isotope dilution was placed in a Vycor crucible and dissolved in HCl. This solution was analyzed by the same procedure as used for sample G. The isotope dilution however was carried out with 0.23875 g. of the solution whose composition is shown in Table V and 0.18085 of the solution shown in Table VI. With this sample, the addition of the Ba^{134} enriched solution described in Table VI made

TABLE IV

Standard Solution for Isotope Dilution of Sample G

Compound	Concentration x 10^4 (g/g solution)	Isotope	Concentration x 10^{19} (Atoms/g solution)
$SrCO_3$	0.8408	Sr 86	7.081
		90	-
Sm_2O_3	0.7678	Sm 151	-
		152	1.764
Nd_2O_3	8.489	Nd 142	20.47
		145	9.172
CsCl	5.724	Cs 133	51.31
		137	-
$Ce(NO_3)_4 \cdot 2NH_4NO_3$	8.120	Ce 142	2.466
		144	-

TABLE V

Standard Solution for Isotope Dilution of Sample H

Compound	Concentration x 10^{-5} (g/g solution)	Isotope		Concentration x 10^{17} (Atoms/g solution)
Sm_2O_3	1.680	Sm	151	-
			152	0.1545
Nd_2O_3	1.603	Nd	142	0.1546
			143	0.6928
CsCl	6.175	Cs	133	2.207
			137	-
$Ce(NO_3)_4 \cdot 2NH_4NO_3$	3.398	Ce	140	0.3501
			142	0.04109

TABLE VI

Isotope Dilution of the Standard Solution of Barium Enriched in Ba^{134}

Isotope	Atoms Added ($\times 10^{17}$)	Mass Spectrometric Ratio Before Isotope Dilution	Mass Spectrometric Ratio after Isotope Dilution	Calc. Conc. $\times 10^{16}$ (Atoms/ml solution)
134	0.03282	1.000	1.000	1.950
136	0.1059	0.1463 ± 0.0013	0.2466 ± 0.0018	0.2852
138	0.9723	0.2990 ± 0.0015	1.259 ± 0.004	0.5630

possible the analysis of the fission product Ba^{138} in the sample.

The other half of this sample together with sample J was used for the extraction of rare-gas fission products by K. Fritze et al. (16). In the present work these samples were combined for the extraction of the ruthenium as discussed in section B (c).

(iv) Treatment of Samples I and K

Samples I and K were only used for the determination of the relative abundances of the fission product isotopes of zirconium and molybdenum. The elements were separated from each of the samples as described in sections B (a) and B (b).

(v) Treatment of Sample L

Sample L was used for isotope dilution of rubidium, strontium, molybdenum and cesium. 1.355$_{01}$ g. of the Mo^{96} enriched MoO_3 solution (Table VIII) were placed in a 50 ml erlenmeyer flask together with 5 ml of distilled HCl. Sample L was dissolved in this solution while cooling the flask in an ice bath to control the rate of dissolution and prevent loss of solution by spattering.

When dissolution was complete, the solution was evaporated to dryness using a heat lamp. The residue was dissolved in a solution containing 0.5 ml distilled HNO_3 and 5 ml distilled HCl. The evaporation and dissolution were repeated using 3 ml of 6N HCl to dissolve the residue. One drop of this solution was used in analyzing the cesium, rubidium and strontium elements with the mass spectrometer.

0.21645 g. of the isotope dilution solution whose composition is shown in Table VII was added to the remainder of the sample. The solution

TABLE VII

Standard Solution for Isotope Dilution of Samples L & M

Compound	Concentration x 10^{-4} (g/g solution)	Isotope	Concentration x 10^{16} (atoms/g solution)
$SrCO_3$	1.546	88	0.5218
		90	-
RbCl*	0.5400	85	0.1940
		87	0.07487
$Ce_2(CO_3)_3$	0.9872	133	3.651
		137	-

*Assume for natural rubidium Rb^{85} = 72.15%, Rb^{87} = 27.85% (32).

Table VIII

Isotope Dilution of Mo^{96} Enriched Solution

Isotope	Atoms Added ($\times 10^{18}$)	Mass Spectrometric Ratio Before Isotope Dilution	Mass Spectrometric Ratio After Isotope Dilution	Concentrat $\times 10^{17}$ (Atom solution
96	1.284	1.000	1.000	2.923
98	1.848	0.02040 ± 0.00053	0.985 ± 0.013	0.0596

was evaporated to dryness and the residue re-dissolved in 6N HCl several times to equilibrate the components of the isotope dilution solution and the fission products. The cesium, rubidium and strontium elements in the solution were analyzed using the mass spectrometer.

The molybdenum was then analyzed by the method described in section B (b).

(vi) Treatment of Sample K

Sample K was used to check the results of the isotope dilution of sample L and also to obtain absolute yields for the ruthenium isotopes.

0.253_{04} g. of the solution whose composition is shown in Table V, 1.226_{85} g. of Mo^{96} enriched MoO_3 solution (see Table VI) and 0.773_{50} g. of the ruthenium solution discussed in the next section d (v) were placed in a distillation flask.

Sample K was dissolved in this solution avoiding any losses due to spattering. After equilibration, a drop of the solution was used in analyzing the cesium, rubidium and strontium elements with the mass spectrometer.

The molybdenum and ruthenium were analyzed by the method discussed in sections B (b) and B (c).

(d) Standard Solutions For Isotope Dilution

(i) Samples G and H

The elements strontium, samarium, cerium, neodymium and cesium were isotope diluted. Spectrapure $SrCO_3$, Sm_2O_3, Nd_2O_3 and CsCl supplied by Johnson, Matthey & Co. Ltd., and analar grade $Ce(IO_3)_4$ $2NH_4IO_3$ supplied by the British Drug House Ltd., were weighed into a 250 ml volumetric flask

and dissolved in acidified water to produce concentrations shown in Tables IV and V.

The appropriate amounts of each of these elements was determined in the following manner. Estimated fission yields along with the number of fissions in the sample determined from the irradiation data and weight of sample were used to calculate the approximate number of atoms of each fission element present in samples G and H. The concentrations shown in Tables IV and V are such that the addition of about 0.25 g. of these solutions would produce measurable changes in the isotopic composition of the fission products when added to the samples G and H respectively.

(ii) Barium For Isotope Dilution of Sample H

Ba^{139} is the only isotope of barium formed in fission that is stable or radioactive with a half-life of more than thirteen days. Natural barium is composed of 71.66% Ba^{138} and only 29.34% of six other stable isotopes. Hence, the absolute fission yield of Ba^{138} can not be easily determined using natural barium as the isotope diluent.

Five milligrams of $BaCO_3$ enriched in the Ba^{134} isotope were obtained from the Oak Ridge National Laboratories. Since the abundant isotope in this was different from that in fission, it was more suitable for the isotope dilution.

The Ba^{134} enriched $BaCO_3$ was dissolved in HCl and the solution diluted to 25 ml in a volumetric flask. Since the $BaCO_3$ obtained from ORNL was of undetermined purity, the concentrations of the barium isotopes in this solution were determined by isotope dilution in the following manner.

0.02221 g. of natural $BaCO_3$ was dissolved in 250 ml of de-ionized distilled H_2O. 0.5 ml of this solution was equilibrated with 5 ml of the

Ba^{134} enriched barium solution by repeatedly evaporating to dryness and re-dissolving the residue in water. A drop of the solution was analysed in the mass spectrometer.

The calculated concentrations of Ba^{134} Ba^{136} and Ba^{138} in the enriched solution are given in Table VI along with the measured mass spectrometric data.

(iii) Standard Solutions For Isotope Dilution of Samples L and M

Spectrum compounds of $SrCO_3$, RbCl and Cs_2CO_3 supplied by Johnson, Matthey & Co. Ltd., were used in the preparation of the standard isotope dilution solution. The procedure was similar to that used for the standard solution (d) (i), the resulting concentrations being given in Table VII.

(iv) Molybdenum

The presence of natural molybdenum in the tungsten of the source in the mass spectrometer filaments prohibited the use of natural elements for isotope diluting fission molybdenum.

MoO_3 was obtained from the Oak Ridge National Laboratories in which the molybdenum had been enriched to 93.2% in Mo^{96}. This was dissolved in NH_4Cl and then diluted to 100 ml in a volumetric flask. Since the purity of this material was uncertain the concentration of this solution was determined by isotope dilution as follows. 0.07712 g. of natural MoO_3 was dissolved in NH_4Cl and the solution diluted to 100 ml with H_2O. 2.4279 g. of this solution was equilibrated with 2.0648 g. of the Mo^{96} enriched solution by repeated evaporations and re-dissolutions. The molybdenum in the solution was analysed with the mass spectrometer. The

isotope dilution data was shown in Table VIII.

(v) Ruthenium

The standard solution for ruthenium isotope dilution was a solution of natural element in HCl. The concentration of the solution was determined by reducing the ruthenium to the metal with Mg metal. After all the ruthenium had been precipitated as the metal, sufficient HCl was added to dissolve any excess Mg. The metallic suspension of ruthenium was filtered and weighed.

The concentration of the ruthenium in the original solution was 0.1240 mg/g. solution.

(E) Determination Neutron Flux and Effective Cross Section

In order to obtain the number of fissions occurring in a sample it is necessary to know the flux and also the effective cross section of the fissile material. The flux can be determined by measuring the extent of neutron capture which occurred in a Co^{59} wire that had been irradiated together with the sample. The Co^{60} can be determined by comparison of its rate of disintegration $\frac{(dN_{60})}{dt}$ to that of Co^{60} standards of known activity. This is accomplished by means of a well-type ionization chamber filled with argon at 30 atmospheres pressure. The ion currents from the ionization chamber are determined with a vibrating-reed electrometer. The cobalt standards had been calibrated previously both by coincidence and 4π counting techniques by the Atomic Energy of Canada Ltd. The integrated flux may be related to the rate of disintegration by equation

(1) Appendix A.

The effective neutron cross section, $\hat{\sigma}$ of any nuclide is a

TABLE IX

Neutron Absorption Rates in Xe^{135}

Sample		Cs^{135}/Cs^{137} Corrected for decay $t_{1/2}$ = 30 yrs	Cs^{135}/Y^{135}	$_{54}\sigma^{135}\phi$ hr^{-1}
B	Top	0.7649 ± 0.0057	0.7334 ± 0.0057	0.03801 ± 0.0011
	Bottom	0.7632 ± 0.0039	0.7317 ± 0.0040	0.03830 ± 0.00075
C	Top	0.4868 ± 0.0021	0.4667 ± 0.0022	0.1308 ± 0.0014
	Bottom	0.4793 ± 0.0027	0.4595 ± 0.0028	0.1355 ± 0.0018

function of the neutron energy distribution and the variation of its cross section with energy and may be calculated by application of equation (2) Appendix A. For non-$\frac{1}{v}$ fissioning nuclides, such as Pu^{239}, the value of the effective fission cross section (σ_f) is also dependent on the apparent neutron temperature. The apparent neutron temperature may be estimated from the change in the $\frac{Sm^{150}}{Sm^{149}}$ ratio in a samarium monitor which had been irradiated with the sample as follows:

Substituting the value of this ratio after irradiation into equation (3) Appendix A, the effective cross section of the Sm^{149} ($\hat{\sigma}_{Sm^{149}}$) may be calculated. Knowing $\hat{\sigma}_{Sm^{149}}$, σ_c and r, the neutron temperature can be estimated by the values of g and s necessary to solve equation 2 and the tables in Westcott (20).

Once the neutron temperature has been established, the effective neutron cross section of the non-$\frac{1}{v}$ fissioning nuclide (Pu^{239}) may be estimated by substituting the g and s values corresponding to this temperature tabulated in Westcott and the 2200m/sec. fission cross section (σ_o) in equation 2.

EXPERIMENTAL RESULTS

(A) Thermal Neutron Absorption Cross Section of Xe^{135}

The $\frac{Cs^{135}}{Cs^{137}}$ ratios measured for the four uranium samples B-top, B-bottom, C-top and C-bottom were corrected for decay of Cs^{137} as shown in column 2, Table IX. These experimental values of $\frac{Cs^{135}}{Cs^{137}}$ divided by the fission yield ratio of 1.043 ± 0.002 previously obtained by Petruska et al. (14) give the ratio of the measured yield of Cs^{135} to the yield when no neutron absorption occurs ($\frac{Cs^{135}}{Y135}$) for each of the four simultaneously irradiated samples. The values of $_{54}\sigma^{135}\phi$ shown in Table IX have been calculated from these $\frac{Cs^{135}}{Y135}$ ratios using equation (4), Appendix B.

In Table X are shown the values of the disintegration rates, measured in the manner discussed in section E of the experimental section, and weights of the cobalt monitors. The effective absorption cross sections of the cobalt shown in column 6 of Table X were calculated (assuming 2200m/sec. absorption cross section of 36.5 barns) in the manner described by Westcott (20) using equation (2), Appendix A. The values of the neutron temperature and the epithermal indices required for this evaluation have been determined by Bigham (33) in connection with this present work. The flux depression or self shielding in the cobalt was calculated as described by Petruska et al. (14). The final column of Table X gives the calculated values of the flux using the irradiation time of 87.83 hours.

TABLE X

Cobalt Monitor Data

Sample	Self-Serve Position	Weight Co^{59} (mg)	Disintegration Rate (counts/sec x 10^7)	Neutrons* temp. °C	σ barns*	Epithermal Index (r)*	ϕ n/cm^2/sec** (x 10^{15})
B Top	5 - 6 - 3	1.134	0.1585 ± 0.0012	137	36.89	0.0098	0.3265 ± 0.0022
Bottom		1.163	0.1591 ± 0.00098				0.3288 ± 0.0015
C Top	5 - 3 - 5	1.163	0.6904 ± 0.0018	120	36.33	0.018	1.141 ± 0.003
Bottom		1.151	0.8123 ± 0.0027				1.238 ± 0.005

*Epithermal indices defined by Westcott (20) and neutron temperatures both measured by Bigham (33).

**Corrected by factor of 0.977 for self-shielding.

TABLE XI

Effective Neutron Absorption Cross Section of Xe^{135}

Sample	Self-Serve Position	Neutron temp. °C	Flux (ϕ) x 10^{13} n/cm^2/sec	σ Xe^{135} (megabarns)	Average σ Xe^{135} (megabarns)
B Top	S - 6 - 3	137	0.3243 ± 0.0022	3.204 ± 0.095	3.27 ± 0.11
Bottom			0.3244 ± 0.0019	3.276 ± 0.068	
C Top	S - 3 - 5	120	1.151 ± 0.0040	3.154 ± 0.034	3.19 ± 0.06
Bottom			1.198 ± 0.0044	3.138 ± 0.042	

In order to obtain the absorption cross section of Xe^{135} from $_{54}\sigma^{135}\phi$ given in Table IX, it was necessary to know the flux in each uranium sample. The flux at each of the uranium positions was interpolated from the values at the cobalt positions given in Table X assuming a linear flux gradient between the monitors in each block assembly. These values corrected for a 0.998 self-shielding factor in the uranium pins are given in Table XI.

The effective neutron absorption cross sections in Table XI were obtained by dividing $_{54}\sigma^{135}\phi$ given in column 4, Table IX by these fluxes.

(B) Thermal Neutron Absorption Cross Section of Sm^{149}

To obtain the effective neutron cross section of Sm^{149} for positions 8-6-3 and 8-3-5 in the NRX reactor, shown in column 6, Table XII, the $\frac{Sm^{150}}{Sm^{149}}$ ratio measured for the irradiated solutions of natural samarium in samples B and C was substituted in equation (3), Appendix A.

The flux in these solutions was estimated by correcting the interpolated values for the cobalt monitors shown in Table X for self-shielding. The effective neutron absorption cross section may be used to evaluate the 2200m/sec. cross section by means of equation (2), Appendix A. Epithermal indices (r) equal 0.0396 and 0.018 and the neutron temperatures 137°C and 120°C were measured by Bigham (33) for positions 8-6-3 and 8-3-5 respectively. The g and s values at those temperatures were obtained from the tables by Westcott (20).

Values of 42,600 barns and 42,500 barns were calculated for σ_o, the cross section of Sm^{149} for 2200m/sec. neutrons.

TABLE XII

The Effective Neutron Absorption Cross Section of Sm^{149}

Sample	Reactor Position	Flux $n/cm^2/sec$	Irradiation Time (days)	Mass Spectrometric Ratio Sm^{149}/Sm^{150}	Cross Section Sm^{149}, barns
B	S - 6 - 3	3.28×10^{12}	5.66	1.475 ± 0.0058	83,800
C	S - 3 - 5	1.19×10^{13}	3.66	0.921 ± 0.006	81,200

(c) Determination of Half-Lives

(i) Strontium-89

The half-life of radioactive Sr^{89} has been determined by observing the change in the ratio of $\frac{Sr^{89}}{Sr^{90}}$ with time. Values obtained from samples A and F are given in Table XIII and shown in Figure 1.

The curves drawn through the data have been calculated by the method of least squares and give half-lives of 52.3 ± 1.0 days for sample A and 51.34 ± 0.97 days for sample F after applying a correction for the decay of Sr^{90}.

(ii) Zirconium-95

The half-life of Zr^{95} was determined using the zirconium separated from sample A. The value of the ratio of $\frac{Zr^{95}}{Zr^{96}}$ was measured from time to time as shown in Table XIV. The curve in Figure 2 which was determined by the method of least squares gave a value of 65.79 ± 0.92 days for the half-life of Zr^{95}.

(D) Relative Yields of the Heavy Mass Fragments in the Thermal Neutron Fission of Pu^{239}

The relative yields of the isotopes of cesium, samarium, neodymium and cerium were determined using the mass spectrometer.

(a) Cesium

The observed mass spectrometric ratios of the cesium isotopes for samples G, H and L are shown in Table XV. To obtain the relative yields of these isotopes it was necessary to correct the Cs^{135} for the loss in the mass 135 chain from neutron absorption by Xe^{135} and the Cs^{137} for the

TABLE XIII

Mass Spectrometric Ratios of Sr^{89}/Sr^{90}

Observation (n)	Sample A		Sample F	
	t (days)	Ratio Sr^{89}/Sr^{90}	t (days)	Ratio Sr^{89}/Sr^{90}
1	0	0.3205 ± 0.0043	0	0.2219 ± 0.0054
2	9.29	0.2605 ± 0.0020	27.82	0.1534 ± 0.0023
3	50.23	0.1647 ± 0.0017	57.0	0.1036 ± 0.0014
4	93.02	0.0900 ± 0.0009	83.90	0.0719 ± 0.0016
5	119.19	0.0666 ± 0.018	-	-
6	153.07	0.0427 ± 0.0073	-	-

TABLE XIV

Mass Spectrometric Ratios of Zr^{95}/Zr^{96}

n	t (days)	Ratio Zr^{95}/Zr^{96}
1	0	0.4418 ± 0.0035
2	43.23	0.2862 ± 0.0047
3	83.94	0.1874 ± 0.0024
4	111.94	0.1358 ± 0.0027
5	140.27	0.1017 ± 0.0014

TABLE XV

Relative Yields of Cesium Isotopes Produced in the Thermal Neutron Fission of Pu^{239}

Sample	Isotope	Time From End of Irradiation (years)	Mass Spectrometric Ratios	Corrected for Neutron Absorption*	Corrected for Decay**	Literature Values	
						Wilson (3)	Krizhanski (4)
G	133	.6986	1.000	1.000	1.000		
	135		0.7765 ± 0.0094	1.05 ± 0.15	1.05 ± 0.15		
	137		0.9233 ± 0.0092	0.9233 ± 0.0092	0.9418 ± 0.0094		
H	133	1.2904	1.000	1.000	1.000		
	135		0.786 ± 0.011	1.04 ± 0.15	1.04 ± 0.15		
	137		0.907 ± 0.013	0.907 ± 0.013	0.939 ± 0.013		
L	133	.2603	1.000	1.000	1.000		
	135		-	-	-		
	137		0.9322 ± 0.0089	0.9322 ± 0.0089	0.9393 ± 0.0089		
Average	133				1.000	1.000	1.000
	135				1.05 ± 0.15	1.05 ± 0.15	2.577 ± 0.240
	137				0.940 ± 0.013	0.994 ± 0.005	2.242 ± 0.020

*Corrected for 3.45×10^6 barn neutron cross section of Xe^{135}.

**Corrected for 26.6 year half-life of Cs^{137}(23).

radioactive decay of Cs^{137} during irradiation and from the end of irradiation to time of analysis. The details of the corrections to the 135 mass chain are given in Appendix C.

The corrected values for the cesium isotope ratios are shown in Table XV.

(b) Samarium

The relative abundances of the samarium isotopes obtained in samples E and G are shown in Table XVII. These ratios were measured as Sm^+ ions. The non-existence of mass 146 indicated the absence of neodymium, hence no neodymium correction was required at mass 150. Under these conditions, it was possible to correct the relative abundances for natural samarium contamination from the amount of mass 148.

Sm^{150} is shielded by stable Nd^{150} and hence the Sm^{150} present after correction for contamination had been formed by neutron absorption of Sm^{149}. The total fission yield of mass 149 was obtained by a summation of the abundances of masses 149 and 150.

The measured abundances of Sm^{147} was corrected since only part of the mass 147 chain had decayed to Sm^{147} from the 2.52 year Pm^{147} at the time of analysis.

The relative abundances of Sm^{151} and Sm^{152} were corrected because of the 12,500 barn neutron capture cross section of Sm^{151} (35). A decay correction was applied to the abundance of 93 year Sm^{151} (36).

The self-shielding factor was calculated for sample G but only approximated for sample F, hence the relative abundances of Sm^{151} and Sm^{152} obtained from sample G were used in later determinations of absolute fission yields.

TABLE XVII

Relative Yields of Samarium Isotopes Produced in the Thermal Neutron Fission of Pu^{239}

Sample	Mass	Mass Spectrometric Ratio	Corrected For Contamination	Corrected For Capture	Corrected For Decay	Relative Yields Literature	
						Wiles (3)	Krizhanski (4)
E	147*	0.1409±0.0021	0.1389±0.0021	0.4565±0.0068	1.846±0.020		
	148	0.01522	-	-	-		
	149	0.3062±0.0021	0.3043±0.0021	1.209±0.011	1.209		
	150	0.06458±0.0081	0.06357±0.00081	-	-		
	151**	0.2194±0.0013	0.2193±0.0013	0.7536±0.0045	0.7536±0.0065		
	152**	0.1839±0.0013	0.1807±0.0013	0.5633±0.0043	0.5633±0.0054		
	154	0.08578±0.00099	0.08274±0.00099	0.2719±0.0032	0.2719±0.0032		
G	147	-	-	-	-		
	148	-	-	-	-		
	149	0.2959±0.0047	0.2959±0.0047	0.4253±0.0085	1.209		
	150	0.1294±0.0025	0.1294±0.0025	-	-		
	151**	0.2464±0.0041	0.2464±0.0041	0.2606±0.0042	0.7410±0.0119		
	152*	0.2151±0.0037	0.2151±0.0037	0.2000±0.0036	0.5685±0.010		
	154	-	-	-	-		
Average	147				1.846±0.020	1.884±0.020	1.838±0.003
	149				1.209	1.209	1.209

TABLE XVII (Continued)

Sample	Mass	Mass Spectrometric Ratio	Corrected For Contamination	Corrected For Capture	Corrected For Decay	Relative Yields Literature Wiles (5)	Literature Zvicharski (4)
Average	151				0.741±0.010	0.736±0.014	0.764±0.01
	152				0.569±0.010	0.595±0.014	0.580±0.01
	154				0.2719±0.0052	0.269±0.006	0.195±0.004

*Corrected for 2.52-year half-life of Pm^{147} (27), time from end of irradiation being 362.4 and 255.7 days respectively.

**Corrected for 12,800 barn cross section of Sm^{151} (35).

(c) Neodymium

The relative yields of the neodymium isotopes occurring in the fission of Pu^{239} were determined using sample C. The abundances were measured as NdO^+ ions. A mass 149 indicated the presence of samarium. Therefore a 1.5% correction obtained from the ratio $\frac{Sm^{149}}{Sm^{150}}$ in the sample was made to the measured abundance of mass 150. The measured abundances of the neodymium isotopes were corrected at each mass for the presence of natural neodymium which corrections were obtained from the amount of Nd^{142}, an isotope not produced in fission. A decay correction was required for mass 144 since the Ce^{144} had not completely decayed to Nd^{144} at the time of analysis.

No correction for neutron absorption by Nd^{143} was necessary for the low integrated flux with which this sample was irradiated. The corrected values are shown in Table XIX.

(d) Cerium

The relative yields of the cerium isotopes in the thermal neutron fission of Pu^{239} were determined for samples F and G from mass spectrometric measurements of the abundances of CeO^+ ions. Since mass 143 was absent, no corrections were required to masses 142 and 144 for neodymium.

Ce^{140} and Ce^{142} isotopes appear in natural cerium as well as in fission cerium. The 99.55% total abundance of these two isotopes in the natural element prohibits the detection of any possible natural contamination in measured fission yields and therefore the only assurance that the values obtained are representative of fission products is the reproducibility of the values obtained from different samples.

The relative yields of the cerium isotopes may be obtained from the mass spectrometric ratios when corrected for the amount of 275 day Ce^{144} that

TABLE XVIII

Relative Yields of the Neodymium Isotopes in the Thermal Neutron Fission of Pu^{239}

Isotope	Time From End of Irradiation (days)	Mass Spectrometric Ratio	Corrected for Contamination	Corrected for Decay	Literature Values	
					Miles (3)	Krizhanski (4)
142*	256.1	0.00792				
143*		1.004	1.000	1.000	1.00	1.00
Nd^{144}**		0.431 ± 0.005	0.424 ± 0.005	0.841 ± 0.010	0.836 ± 0.006	0.840 ± 0.006
Nd^{145}		0.687 ± 0.008	0.685 ± 0.008	0.685 ± 0.008	0.681 ± 0.002	0.666 ± 0.002
Nd^{146}		0.568 ± 0.008	0.563 ± 0.008	0.563 ± 0.008	0.561 ± 0.005	0.557 ± 0.002
Nd^{148}		0.377 ± 0.008	0.375 ± 0.006	0.375 ± 0.006	0.379 ± 0.002	0.362 ± 0.005
Nd^{150}		0.225 ± 0.003	0.223 ± 0.003	0.223 ± 0.003	0.219 ± 0.002	0.220 ± 0.002

*Correction for 334 barn neutron absorption cross section of Nd^{143} was insignificant in this work (37).

**Corrected for 278-day half-life of Ce^{144}.

has decayed through Pr^{144} to Nd^{144} during this irradiation and the time from the end of the irradiation to the time of analysis. The relative yields of Ce^{140}, Ce^{142} and Ce^{144} are shown in Table XI together with the observed mass spectrometric ratios.

(E) Absolute Fission Yields of Ba^{136}, Cerium, Samarium, Cesium and Neodymium Isotopes

The isotope dilution data along with the evaluated number of atoms of Ce^{142}, Sm^{149}, Cs^{133} and Nd^{143} per gram of plutonium in each sample, G and H are contained in Tables XX to XXIII. From the relative yields for each of the elements given in Tables XIV, XVII, XVIII and XIX and the absolute number of atoms of one isotope of each of the elements given in Tables XX to XXIII the number of atoms per gram of plutonium have been tabulated in columns 2 and 4 of Table XXV.

The yield of Ba^{138} was determined only for the Pu-Al alloy sample using the isotope dilution data shown in Table XXIV. The isotope dilution data and calculated number of fission atoms of Ba^{138} per gram of plutonium are given in Tables XXIV and the final value shown with those for the other fission products in Table XXV.

The yields of the xenon isotopes given by Fleming and Thode (38) were normalized to the cesium isotopes by means of the factor 0.925 ± 0.010 given by those authors for the ratio of $\frac{Xe^{133}}{Xe^{134}}$. In the mass region below mass 130, radiochemical yields have been used where possible. Other yields appearing in Table XXV including masses 139 and 141, which have not been obtained directly, have been interpolated from a plot of yield versus mass.

The yield of the 144 mass chain may be obtained both from the cerium and neodymium isotope dilutions. For sample G, the value obtained from the neodymium is 15% higher than from the cerium. It may be seen from Table XXIII that for this sample too much natural neodymium had been used

TABLE XIX

Relative Yields of the Cerium Isotopes in Thermal Neutron Fission of Pu^{239}

Sample	Isotope	Time From End of Irradiation (days)	Mass Spectrometric Ratio	Corrected for Decay	Literature Values	
					Wiles (3)	Krizhanski (4)
F	140	216.5	1.127 ± 0.007	1.127 ± 0.007		
	142		1.000	1.000		
	144		0.4083 ± 0.0029	0.7777 ± 0.0095		
G	140	255.7	1.124 ± 0.0075	1.124 ± 0.007		
	142		1.000	1.000		
	144		0.3834 ± 0.0032	0.7730 ± 0.0050		
Average	140			1.126 ± 0.007	1.11 ± 0.02	0.85 ± 0.01
	142			1.00	1.00	1.00
	144			0.7738 ± 0.0060	0.77 ± 0.02	0.79 ± 0.04

TABLE XX

Mass Spectrometric and Isotope Dilution Data For Ce^{142} Produced in the Thermal Neutron Fission of Pu^{239}

Sample	Isotope	Ratio Before Isotope Dilution	No. of Atoms added per g of Pu^{239} (x 10^{18})	Ratio After Isotope Dilution	Calculated Fission Yield (Atoms x 10^{17}/g Pu^{239})
G	140	-	-	-	-
	142	1.000	2.052	1.000	9.880
	144	0.3694 ± 0.0031	-	0.09501 ± 0.00080	-
H	140	1.000	1.491	1.000	-
	142	0.6668 ± 0.0051	0.1865	0.3204 ± 0.0030	5.299
	144	-	-	-	-

TABLE XXI

Mass Spectrometric and Isotope Dilution Data For Sm^{151} Produced in the Thermal Neutron Fission of Pu^{239}

Sample	Isotope	Ratio Before Isotope Dilution	No. of Atoms added per g of Pu^{239} (x 10^{18})	Ratio After Isotope Dilution	Calculated Fission Yield (Atoms x 10^{17}/g Pu^{239})
G	151	1.000	-	1.000	1.642
	152	0.8705 ± 0.0181	0.4766	13.95 ± 0.040	-
H	151	1.000	-	1.000	0.8313
	152	0.8646 ± 0.0107	0.1957	0.1029 ± 0.0019	-

TABLE XXII

Mass Spectrometric and Isotope Dilution Data For Cs^{133} Produced in the Thermal Neutron Fission of Pu^{239}

Sample	Isotope	Ratio Before Isotope Dilution	No. of Atoms added per g of Pu^{239} ($\times 10^{19}$)	Ratio After Isotope Dilution	Calculated Fission Yield (Atoms $\times 10^{18}$/g Pu^{239})
G	133	1.000	5.932	1.000	1.405
	137	0.923 ± 0.013	-	0.0214 ± 0.0003	-
H	133	1.000	0.3970	1.000	0.7193
	137	0.907 ± 0.013	-	0.0611 ± 0.0004	-

TABLE XXIII

Mass Spectrometric and Isotope Dilution Data For Nd^{143} Produced in the Thermal Neutron Fission of Pu^{239}

Sample	Isotope	Ratio Before Isotope Dilution	No. of Atoms added per g of Pu^{239} (x 10^{18})	Ratio After Isotope Dilution	Calculated Fission Yield (Atoms x 10^{18}/g Pu^{239})
G	142	-	2.366	2.026 ± 0.015	-
	143	1.000	1.060	1.000	1.076
H	142	-	0.6984	0.8744 ± 0.0078	-
	143	1.000	0.3130	1.000	4.856

TABLE XXIV

Mass Spectrometric and Isotope Dilution Data For Ba^{138} Produced in the Thermal Neutron Fission of Pu^{239}

Sample	Isotope	Ratio Before Isotope Dilution	No. of Atoms added per g of Pu^{239} (x 10^{17})	Ratio After Isotope Dilution	Calculated Fission Yield (Atoms x 10^{17}/g Pu^{239})
H	134	-	6.486	0.2484 ± 0.0025	-
	136	-	0.9485	0.1097 ± 0.0019	-
	138	1.000	1.940	1.000	6.575

in the isotope dilution so that the ratio of $\frac{Nd^{142}}{Nd^{143}}$ after isotope dilution was very nearly that of natural neodymium. For such conditions the accuracy of the determination of the number of fission Nd^{143} is greatly reduced. In Table XXIII therefore the values for the neodymium isotopes in sample G have been obtained from the relative yields shown in Table XXIII and the number of atoms of mass 144 taken from Ce^{142} shown in Table XX. For the plutonium-aluminum alloy, sample H, identical yields at mass 144 were obtained from both the cerium and neodymium isotope dilutions. This agreement is obtained when a value of 278 day half-life for Ce^{144} is assumed for the growth and decay corrections of the observed mass spectrometric data of both the neodymium and cerium given in Tables XVIII and XIX respectively.

Two methods may be used to obtain the absolute cumulative fission yields from the data given in columns 2 and 4 of Table XXV. In one method the absolute number of fissions is calculated from the irradiation data and the fission cross section of Pu^{239}, and in the other method the relative yields are adjusted so that they total 100%. The absolute number of fissions may be calculated using equation (7) in Appendix E. The integrated flux and the effective neutron fission cross section required for the determination of the number of fissions are obtained from the cobalt and the samarium monitors according to the method described in section A.

For the cobalt monitors, the r value was taken as 0.01, σ_0 = 36.5 barns (39), $\lambda = 4.18 \times 10^{-9} sec^{-1}$ and 123°C for the apparent temperature of the Maxwellian component of the neutron distribution. Using the values of g and s taken from tables given by Westcott (20) a value

of 36.9 barns was obtained for the effective neutron cross section of Co^{59}. Using the methods previously described by Petruska et al. (14), 0.977 self-shielding corrections were made for the cobalt monitors. With these quantities the measured specific activities of the cobalt monitors shown in Table XXVI, the values of the neutron flux shown in Table XXVI have been calculated using equation (1), Appendix A.

The value of the effective fission cross section, $\hat{\sigma}_f$ for Pu^{239} is dependent on the apparent neutron temperature. The apparent neutron temperature may be calculated from the effective cross section of Sm^{149} as shown in section A (b).

For the plutonium-aluminum alloy sample H, the observed value of $\frac{Sm^{150}}{Sm^{149}}$ was found to be 1.35 ± 0.01 and hence $\hat{\sigma}_{Sm^{149}}$ = 81,500 barns. A value of 123°C for the neutron temperature was estimated from equation (2) using 42,200 barns for $\hat{\sigma}_o$ (35), r = 0.01 and values of g and s given as a function of temperature by Westcott (20). For this temperature a value of 572 barns is estimated for the effective fission cross section of Pu^{239} from equation (3) using 750 barns for the 2200m/sec. fission cross section and the values of g and s tabulated by Westcott (20).

Although the PuO_2 sample did not have a samarium monitor, it was irradiated in the same position in the BNL reactor and the fission cross sections for plutonium has been assumed to have the same value. With this value for the effective fission cross section of Pu^{239}, the self-shielding corrections calculated in the same manner as for the cobalt monitors and the integrated fluxes given in Table XXVI, the number of fissions per gram of plutonium shown in this table have been calculated using equation (7), Appendix B.

TABLE XXV

Cumulative Yields For Pu^{239} Based on the Calculated Number of Fissions

Mass Chain	PuO_2 No. of Atoms/ g Pu^{239} ($\times 10^{18}$)	PuO_2 % Yield	Pu-Al Alloy No. of Atoms/ g Pu^{239} ($\times 10^{17}$)	Pu-Al Alloy % Yield
128 - 130		5.697*		5.704*
131	0.7666	5.831	5.925	5.697
132	1.070	5.344	5.477	5.158
133	1.405	7.019	7.195	6.774
134	1.519	7.588	7.775	7.322
135	1.477	7.379	7.552	7.112
136	1.349	6.743	6.907	6.505
137	1.320	6.599	6.763	6.369
138		6.427*	6.574	6.191*
139		6.050*	-	5.92*
140	1.110	5.549	5.955	5.607
141		5.142		5.31*
142	0.9880	4.937	5.299	4.991
143	0.9081	4.537	4.856	4.573
144	0.7637	3.816	4.090	3.850
145	0.6220	3.108	3.326	3.132
146	0.5113	2.555	2.734	2.575
147	0.4075	2.035	2.062	1.942
148	0.3405	1.702	1.822	1.716
149	0.2667	1.333	1.350	1.271
150	0.2025	1.012	1.083	1.020
151	0.1642	0.8206	0.8313	0.7829
152	0.1261	0.6302	0.6383	0.6011
153		0.454*		0.451*
154	0.06001	0.300	0.3038	0.2861
155		0.177*		0.1726*
156		0.081*		0.0833*
TOTAL		100.86%		99.13%

*Assumed Yields.

with the yields in atoms per gram of plutonium given in columns 2 and 4 of Table XIV and the number of fissions per gram of plutonium given in Table XVI, the yields shown in columns 3 and 5 in Table XIV have been obtained.

The method of adjusting the absolute cumulative yields of the heavy mass fission products to add to 100% is accomplished by taking the ratios of 100 times the number of atoms per gram of plutonium which is given in columns 2 and 4 of Table XIV to the total number of fissions per gram of plutonium which are given in column 2 and 4 of Table XIV to the total number of fissions which are the summations of columns 2 and 4 of Table XIV.

The final fission yields shown in Table XVII have been obtained in this manner.

(F) Light Mass Yields of Pu^{239}

The relative yields of the isotopes of rubidium, strontium, yttrium, zirconium, molybdenum and ruthenium were determined with the mass spectrometer as described in the experimental section.

(a) Rubidium

Since Rb^{85} and Rb^{87} are the only isotopes that occur in nature and also in fission product (i.e. with $t_{\frac{1}{2}} > 17.8$ minutes) the possibility of contamination by the natural isotopes always arises in the fission product abundance measurements. Therefore, as in the case of cerium, the only assurance that the values obtained are representative of fission products is the reproducibility of the values obtained for different samples.

TABLE XXVI

Number of Fissions in the Plutonium Sample

Sample	Specific Activity of Cobalt Monitors mc/g	(nv)t n/cm^2	Self-Shielding Correction	Number of Fission/g of Pu^{239}
C	650.7	1.525×10^{19}	0.6043	2.001×10^{19}
H	216*	5.19×10^{18}	0.930	1.062×10^{18}

*Average for two monitors.

To obtain the actual fission yield of Rb^{85}, a correction was made since the parent nuclide Kr^{85} has two isomers. 23.0% of the total yield decays through the 10.27 yr. isomer while 77.0% decays through the 4.36 hr. isomer (40). Thus the measured Rb^{85} represented 77.0% of the yield together with a fraction of the remaining 23.0% depending on the time of analysis.

The measured ratio $\frac{Rb^{85}}{Rb^{87}}$ was 0.4517 ± 0.0036. A fission yield ratio of 0.5872 ± 0.0050 was obtained after correcting the Rb^{85} for the decay of Kr^{85} during irradiation and the 0.3535 years from the end of irradiation to the time of analysis.

(b) Strontium

Three isotopes of strontium having $t\frac{1}{2} > 9.7$ hrs. appear in fission, namely Sr^{88}, Sr^{89} and Sr^{90}. In nature, four stable isotopes exist, Sr^{84}, Sr^{86}, Sr^{87} and Sr^{88}, the latter having 82.56% abundance.

Thus a correction can be made to fission Sr^{88} for natural contamination through the 9.86% Sr^{86} although a small error in the measurement of Sr^{86} makes a considerable error in the correction to Sr^{88}.

Measured mass spectrometric ratios of the strontium isotopes are given in Table XLVIII, together with the ratios after contamination correction, if any, and the decay corrections for Sr^{89} and Sr^{90} have been made.

(c) Zirconium

Fission zirconium was separated from the fission products by dialysis as discussed in section (B) (b). Two samples were separated

TABLE XXVII

Cumulative Yields of the Heavy Mass Fragments Formed in the Fission of Pu^{239} Together With Literature Values

Mass Chain	PuO_2 % Yield	Pu-Al alloy % Yield	Average % Yield	Wiles (3) % Yield	Steinberg et al. (2) % Yield
118 - 130	5.65*	5.75*	5.70*	5.38*	
131	3.80	3.73	3.77	2.71	3.6
132	5.30	5.21	5.26	3.79	4.9
133	6.96	6.83	6.90	4.97	5.0
134	7.52	7.39	7.46	5.37	
135	7.32	7.17	7.25	5.22	5.5
136	6.69	6.56	6.62	4.77	
137	6.54	6.42	6.48	4.94	5.8
138	6.37*	6.25	6.31	5.38	
139	6.00*	5.97*	5.99*	6.61*	5.4
140	5.50	5.66	5.58	7.36	5.36
141	5.10*	5.36*	5.23*	6.94	4.9
142	4.90	5.03	4.97	6.62	
143	4.50	4.61	4.56	5.98	5.1
144	3.78	3.89	3.84	5.00	3.7
145	3.08	3.16	3.12	4.07	
146	2.53	2.60	2.57	3.36	
147	2.02	1.96	1.99	2.81	
148	1.69	1.73	1.71	2.27	
149	1.32	1.28	1.30	1.81	
150	1.00	1.03	1.02	1.31	
151	0.814	0.790	0.802	1.10	
152	0.625	0.606	0.616	0.88	
153	0.45*	0.45*	0.45*	0.64	0.39
154	0.297	0.289	0.293	0.40	
155	0.17*	0.17*	0.17*	0.30	
156	0.08*	0.08*	0.08*	0.08	0.12
TOTAL	100%	100%	100%	100%	93%**

*Assumed yields.

**Summation of measured yields together with values interpolated from smooth mass-yield curve by Steinberg and Freedman (2) totalling 93%.

and analyzed; sample E was analyzed using a single filament source and sample I using the multiple filament source. In the former case, the relative yields of the zirconium isotopes were measured as the Zr^{+} ions, in the latter as the ZrO^{+} ions.

Stable Zr^{90} occurs in nature but not in young fission products since Sr^{90}, a precursor in the decay chain, has a half-life of 27.7 years. Thus the Zr^{90} yield after correcting for Sr^{90} decay, if necessary, was used to estimate the natural contamination to Zr^{91}, Zr^{92}, Zr^{94} and Zr^{96} yields.

It should be noted that the decay times used for the correction of the measured yields of Zr^{91} and Zr^{95} were not the same. The decay time for Zr^{95} represents the time until the mass spectrometric analysis. However, in the case of the Zr^{91} which is growing in through its 56.0 day Y^{91} precursor, the decay time only includes the time until the dialysis of the sample.

The resulting relative yields of the zirconium isotopes of masses 91-96 are shown in Table XXII along with the measured mass spectrometric data.

For sample E, a large correction was required to obtain the Zr^{91} yield from the measured Zr^{91} since a large fraction of this chain had not decayed from Y^{91}. This correction required a knowledge of the time of separation of the zirconium from the yttrium, which by dialysis required several days. An estimate of the yield of Zr^{91} has therefore not been shown for this sample.

On the other hand, for sample I the time of dialysis and half-life of the Y^{91} precursor were not critical in correcting the abundance of Zr^{91} since the sample had decayed for over a year. This sample, however, gave essentially no Zr^{95}.

TABLE XXVIII

Relative Yields of Strontium Isotopes in the Thermal Neutron Fission of Pu^{239}

Sample	Time From End of Irradiation	Isotope	Mass Spectrometric Ratio	Corrected For Contamination	Corrected For Decay
F	70.78 days	86	0.02667 ± 0.00009	-	-
		88	0.8713 ± 0.018	0.6482 ± 0.0133	0.644 ± 0.013
		89	0.2212 ± 0.0025	0.2212 ± 0.0025	0.7846 ± 0.0089*
		90	1.000	1.000	1.000**
L	57.0 days	86	-	-	-
		88	0.6590 ± 0.0062	0.6590 ± 0.0062	0.6550 ± 0.0062
		89	-	-	-
		90	1.000	1.000	1.000**

*$t_{1/2}$ for Sr^{89} = 51.8 days.

**$t_{1/2}$ for Sr^{90} = 27.7 years (41).

(d) Yttrium

The ratio of $\frac{Y^{91}}{Y^{89}}$ was determined using sample F. Difficulties arise in obtaining the relative yields of these isotopes not because of uncertainties in the ratios measured with the mass spectrometer but because of the uncertainty in the decay corrections which are necessary. The Y^{89} is formed from the Sr^{89} precursor whose 51.8 day half-life was measured in this work. However, the reported half-life of Y^{91} is not as well established. In the calculation of the relative yields, the value of 58 days (42), (43) has been used for the half-life of Y^{91}.

The measured mass spectrometric ratios of Y^{89} and Y^{91} together with the relative yields obtained using these half-lives are shown in Table XXX.

(e) Molybdenum

The analysis of the fission molybdenum present in a sample was complicated by the fact that both tantalum and tungsten filaments contain small amounts of natural molybdenum. Thus in order to determine the operating conditions of the mass spectrometer for observing the molybdenum in a sample, it was necessary to use molybdenum of a different isotopic composition than the natural molybdenum in the filament.

50 mg of MoO_3 enriched to 93.2% in Mo^{96} was obtained from Oak National Laboratories. In analyzing fission molybdenum, only masses 95, 97, 98 and 100 are observed, thus mass 96 can be used to correct these relative yields for natural contamination.

It was also necessary to correct the measured abundance of Mo^{95} for the amounts of Zr^{95} and Nb^{95} which have not yet decayed to Mo^{95}. For

TABLE XXX

Relative Yields of Yttrium Isotopes in the Thermal Neutron Fission of Pu^{239}

Isotope	Time From End of Irradiation (days)	Mass Spectrometric Ratio	Corrected For Decay
89	70.80	1.000	1.00
91		0.6433 ± 0.0098	1.44 ± 0.02
89	98.4	1.000	1.00
91		0.4156 ± 0.0066	1.44 ± 0.02

$t_{1/2}$ for Sr^{89} = 51.8 days.

$t_{1/2}$ for Y^{91} = 58 days.

sample K this correction was too large for an accurate estimation of the mass 95 yield.

The measured mass spectrometric abundances and the relative yields are given in Table XXII.

(f) Ruthenium

The ruthenium extracted from sample J together with $\frac{1}{2}$ sample H was analysed on the mass spectrometer. The absence of mass 99 proved that no natural ruthenium was present as a contaminant.

The measured abundances of masses 101, 102, 104 and 106 in the fission product samples together with the relative yields after correction for the decay of Ru^{106} are shown in Table XXIII. The Ru^{103} yield was too small to be measured with any degree of accuracy. However, after sample M had been isotope diluted, the relative abundances 103, and 106 were measured.

Since the estimation of the relative yields from these measurements requires the knowledge of two half-lives, that of mass 103 not being well-known, the final relative yield is probably not as accurate as the mass spectrometric precision would indicate.

(C) Absolute Fission Yields of Rubidium, Strontium, Zirconium, Molybdenum and Ruthenium Isotopes.

Table XXXIII contains a summary of the relative yields of the various elements which were used in the determination of absolute fission yields of the light mass fission fragments. The values which were taken from Tables XXVIII, XXIX, XXX, and XXXI are averages weighted according to the inverse square of the standard deviations.

TABLE XXXI

Relative Yields of Molybdenum in the Thermal Neutron Fission of Pu^{239}

Sample	Time from End of Irradiation (days)	Isotope	Mass Spectrometric Ratio	Corrected For Contamination	Corrected For Decay
G	147.73	95	0.790 ± 0.022	0.695 ± 0.022	0.711 ± 0.022*
		96	1.008	-	-
		97	0.856 ± 0.014	0.797 ± 0.014	0.797 ± 0.014
		98	0.969 ± 0.018	0.824 ± 0.018	0.824 ± 0.018
		100	1.059	1.000	1.000
K	84	95	-	-	-
		96	0.3490	-	-
		97	0.994 ± 0.017	0.794 ± 0.017	0.794 ± 0.017
		98	1.335 ± 0.015	0.832 ± 0.015	0.832 ± 0.015
		100	1.204	1.000	1.000

*Assuming 65.6-day half-life for Zr^{95} and 35-day half-life for Nb^{95} (44)(45).

TABLE XXXII

Relative Fission Yields of Ruthenium Isotopes in Fission of Pu^{239}

Sample	Time From End of Irradiation (days)	Isotope	Mass Spectrometric Ratio	Corrected For Decay
J	668.0	101	1.000	1.000
1/2 H	664.1	102	1.013 ± 0.014	1.013 ± 0.014
		104	1.003 ± 0.014	1.003 ± 0.014
		106	0.215 ± 0.075	0.773 ± 0.027
M	92	103	0.1151 ± 0.0019	0.9601 ± 0.0156
		104	1.000	-
		106	0.4345 ± 0.0053	0.7730 ± 0.0093

Average $t_{1/2}$ for Ru^{103} = 39.7 days (49).

Average $t_{1/2}$ for Ru^{106} = 1.01 years (47)(48).

TABLE XXXIII

Relative Yields of Isotopes of Various Light Fragments in the Thermal Neutron Fission of Pu^{239}

Isotope	Relative Yield
Rb^{85}	0.5872 ± 0.0050
Rb^{87}	1.000
Sr^{88}	0.6530 ± 0.0071
Sr^{89}	0.7846 ± 0.0089
Sr^{90}	1.000
Y^{89}	1.000
Y^{91}	1.44 ± 0.02
Zr^{91}	0.6591 ± 0.0093
Zr^{92}	0.790 ± 0.020
Zr^{93}	1.000
Zr^{94}	1.129 ± 0.017
Zr^{95}	1.266 ± 0.022
Zr^{96}	1.301 ± 0.018
Mo^{95}	0.711 ± 0.022
Mo^{97}	0.796 ± 0.015
Mo^{98}	0.829 ± 0.016
Mo^{100}	1.000
Ru^{101}	1.000
Ru^{102}	1.013 ± 0.014
Ru^{103}*	0.960
Ru^{104}	1.003 ± 0.014
Ru^{106}	0.773 ± 0.027

*See section F(f) for accuracy of this relative yield.

Samples G, L and H were utilized in the determination of the absolute yields of the light fission fragments. The isotope dilution data along with the evaluated number of atoms of Cs^{133}, Rb^{87}, Sr^{90}, Mo^{98} and Ru^{101} per gram of plutonium in each sample are shown in Tables XXXIV to XXXVIII. From the relative yields for each of the elements given in Table XXXIII and the absolute number of atoms of one isotope of each of the elements given in Tables XXXIV to XXXVIII, the number of atoms per gram of plutonium have been tabulated in columns 2, 4 and 6 of Table XXXIX for each of the samples.

The absolute yields of the zirconium isotopes were normalised to the molybdenum through the mass 95 chain. In a similar manner, the relative yields of fission krypton isotopes given by Fritze et al. (16) were normalized to the rubidium isotopes through the yield of the mass 85 chain which was determined by isotope dilution.

For each of the three samples, the number of atoms of Cs^{133} per gram of plutonium was determined. Since the absolute yield of Cs^{133} has been evaluated as 6.90% in section E, it was possible to normalize the atom yields of the isotopes of the other elements to percent yields.

The final values of the measured yields shown in Table XXXIX are the averages of columns 3, 5 and 7. Radiochemical yields for masses 109, 111 and 112 tabulated by Katcoff (17) have been used. All other yields were obtained by interpolation and extrapolation.

(B) Relative Fission Yields in the Thermal Neutron Fission of U^{235}

(a) Strontium

The relative yields of the strontium isotopes formed in the

TABLE XXXIV

Mass Spectrometric and Isotope Dilution Data For Rb^{87} Produced in the Thermal Neutron Fission of Pu^{239}

Sample	Isotope	Ratio Before Isotope Dilution	No. of Atoms of Isotope added per g of Pu^{239} ($\times 10^{18}$)	Ratio After Isotope Dilution	Calculated Fission Yield (Atoms $\times 10^{18}$/ g Pu^{239})
M	85	1.000	4.736	1.000	-
	87	2.202 ± 0.017	1.828	0.6374 ± 0.0032	2.068
L	85	1.000	4.198	1.000	-
	87	2.199 ± 0.017	1.620	0.7706 ± 0.0052	2.472

TABLE XXXV

Mass Spectrometric and Isotope Dilution Data For Cs^{133} Produced in the Thermal Neutron Fission of Pu^{239}

Sample	Isotope	Ratio Before Isotope Dilution	No. of Atoms of Isotope Added per g of Pu^{239} (x 1019)	Ratio After Isotope Dilution	Calculated Fission Yield (Atoms x 1018/ g Pu^{239})
K	133	1.000	5.936	1.000	16.01
	137	0.9329 ± 0.0089	-	0.1421 ± 0.0008	-
L	133	1.000	7.853	1.000	18.35
	137	0.9322 ± 0.0089	-	0.1765 ± 0.0010	-
G	133	1.000	5.938	1.000	1.145
	137	0.9233 ± 0.0135	-	0.02144 ± 0.00028	-

TABLE XXXVI

Mass Spectrometric and Isotope Dilution Data For Sr^{90} Produced in the Thermal Neutron Fission of Pu^{239}

Sample	Isotope	Ratio Before Isotope Dilution	No. of Atoms of Isotope Added per g of Pu^{239} (x 10^{19})	Ratio After Isotope Dilution	Calculated Fission Yield (Atoms x 10^{18}/ g Pu^{239})
H	88	0.6595 ± 0.0062	1.274	3.307 ± 0.022	-
	90	1.000	-	1.000	4.846
L	88	0.6599 ± 0.0062	1.122	2.595 ± 0.011	-
	90	1.000	-	1.000	5.849
G	88	1.191 ± 0.012	0.6678	1.975 ± 0.035	-
	90	1.000	-	1.000	0.3656

TABLE XXXVII

Mass Spectrometric and Isotope Dilution Data For Mo^{98} Produced in the Thermal Neutron Fission of Pu^{239}

Sample	Isotope	Ratio Before Isotope Dilution	No. of Atoms of Isotope Added per g of Pu^{239} (x 10^{19})	Ratio After Isotope Dilution	Calculated Fission Yield (Atoms x 10^{18}/ g Pu^{239})
M	96	-	3.461	1.000	-
	97	0.793 ± 0.019	0.0483	0.3957 ± 0.0034	-
	98	0.830 - 0.017	0.071	0.4429 - 0.0066	13.50
L	96	-	3.878	1.000	-
	97	0.793 ± 0.019	0.0541	0.5045 ± 0.010	-
	98	0.830 ± 0.017	0.079	0.4149 ± 0.0083	15.60

Analysis of enriched solution	Mo^{96}	0.932 ± 0.002
	Mo^{97}	0.013 ± 0.005
	Mo^{98}	0.019 ± 0.01

TABLE XXXVIII

Mass Spectrometric and Isotope Dilution Data For Ru^{101} Produced in the Thermal Neutron Fission of Pu^{239}

Sample	Isotope	Ratio Before Isotope Dilution	No. of Atoms of Isotope Added per g of Pu^{239} (x 10^{18})	Ratio After Isotope Dilution	Calculated Fission Yield (Atoms x 10^{18}/ g Pu^{239})
N	99	-	6.976	0.3042 ± 0.0046	-
	101	1.000	9.338	1.000	13.60

TABLE XXXIX

Cumulative Fission Yields of the Light Fragments in the Thermal Neutron Fission of Pu^{239} Normalized to the 6.90% Cs^{137} Yield

Isotopic Mass	Sample G atoms x 10^{18}	Sample G % Yield	Sample L atoms x 10^{18}	Sample L % Yield	Sample M atoms x 10^{18}	Sample M % Yield	Average % Yield
72 - 82							0.59*
Kr^{83}							0.29
Kr^{84}							0.47
Rb^{85} (Kr^{85})			1.460	0.5456	1.262	0.535	0.535
Kr^{86}							0.75
Rb^{87}			2.487	0.9291	0.2150	0.8942	0.912
Sr^{88}	0.2387	1.458	3.819	1.440	3.164	1.368	1.43
Sr^{89}	0.2868	1.728	4.589	1.726	3.802	1.639	1.71
Sr^{90}	0.3656	2.203	5.849	2.199	4.846	2.089	2.16
Zr^{91}							2.60
Zr^{92}							3.12
Zr^{93}							3.94
Zr^{94}							4.45
Mo^{95} (Zr^{95})			13.37	5.025	11.58	4.991	4.99
Zr^{96}							5.13
Mo^{97}			14.97	5.630	12.97	5.590	5.61
Mo^{98}			15.60	5.861	13.50	5.818	5.84
99							6.44*

TABLE XXXIX (Continued)

Isotopic Mass	Sample G atoms x 10^{18}	Sample G % Yield	Sample L atoms x 10^{18}	Sample L % Yield	Sample M atoms x 10^{18}	Sample M % Yield	Average % Yield
Mo^{100}			1.882	7.072	1.629	7.020	7.05
Ru^{101}					13.60	5.860	5.86
Ru^{102}					13.78	5.939	5.94
Ru^{103}					13.06	5.626	5.63
Ru^{104}					13.64	5.877	5.88
Ru^{105}							5.50*
Ru^{106}					1.051	4.530	4.53
107							3.40*
108							2.44*
109							1.50**
110							0.76*
111							0.27**
112							0.10**
113							0.080*
114							0.060*
115							0.041*
116-118							0.122*
Cs^{133}	1.45	6.90	18.35	6.90	16.01	6.90	
					TOTAL % YIELD		100.13

*Interpolated values.

** Radiochemical yields.

fission of U^{235} were determined from sample A.

The abundance of Sr^{88} was corrected for natural strontium contamination as in section F (b) through the relative amount of mass 86 present, and the yields of masses 89 and 90 were obtained by correction of the observed abundances for radioactive decay. The observed mass spectrometric data and relative fission yields are shown in Table XL.

(b) Yttrium

The ratio of Y^{89} and Y^{91} was also determined from sample A. The irradiation data together with the relative yields are shown in Table XLI.

(c) Neodymium

The relative yields of samarium isotopes were determined from sample A. The presence of mass 142 indicated natural neodymium contamination and hence the appropriate corrections were made to the measured abundances. Mass 150 was also corrected for the presence of fission samarium through mass 149. A value of 0.210 had been obtained for the $\frac{Sm^{150}}{Sm^{149}}$ ratio previous to the appearance of neodymium.

The mass spectrometric ratios together with the relative fission yields are shown in Table XLII.

(d) Zirconium

The relative yields of the isotopes of fission zirconium were determined from samples A and B. The yield of Zr^{95} was determined from the younger sample A and that of Zr^{91} from the older sample B.

The mass 90 was used to correct the abundances of the fission

TABLE XI

Relative Yields of the Strontium Isotopes in the Thermal Neutron Fission of U^{235}

Sample	Time From End of Irradiation (days)	Isotope	Mass Spectrometric Ratio	Corrected For Contamination	Corrected For Decay
A-1	58.2	86	-	-	-
		88	-	-	-
		89	0.3221 ± 0.0041	0.3221 ± 0.0041	0.807 ± 0.010
		90	1.000	1.000	1.000
A-2	108.4	86	0.02158	-	-
		88	0.802 ± 0.017	0.622 ± 0.013	0.622 ± 0.013
		89	0.1627 ± 0.0018	0.1627 ± 0.0018	0.7972 ± 0.0087
		90	1.000	1.000	1.000

$t_{1/2}$ Sr^{89} = 51.8 days.

$t_{1/2}$ Sr^{90} = 27.7 years (41).

TABLE XVI

Relative Yields of the Yttrium Isotopes in the Thermal Neutron Fission of U^{235}

Sample	Time From End of Irradiation (days)	Isotope	Mass Spectrometric Ratio	Corrected For Decay
A-1	60.7	89	1.000	1.000
		91	0.7463 ± 0.019	1.269 ± 0.031
A-2	108.7	89	1.000	1.000
		91	0.7381 ± 0.0070	1.268 ± 0.012

$t_{1/2}$ Y^{91} = 58 days (42)(43).

$t_{1/2}$ Sr^{89} = 51.6 days.

TABLE XLII

Relative Yields of the Neodymium Isotopes in the Thermal Neutron Fission of U^{235}

Isotope	Time From End of Irradiation (days)	Mass Spectrometric Ratio	Corrected For Pd Contamination	Corrected For Sm Contamination	Corrected For Decay
142	260.3	0.01852	-	-	-
143**		1.000	1.000	1.000	1.000
144*		0.4960 ± 0.012	0.480 ± 0.012	0.480 ± 0.012	0.928 ± 0.022
145		0.672 ± 0.010	0.667 ± 0.010	0.667 ± 0.010	0.667 ± 0.010
146		0.5157 ± 0.0097	0.504 ± 0.0097	0.504 ± 0.0097	0.504 ± 0.0097
148		0.2849 ± 0.002	0.281 ± 0.002	0.281 ± 0.0020	0.281 ± 0.0020
149		0.1980	0.1980	-	-
150		0.1557 ± 0.0042	0.1416 ± 0.0038	0.110 ± 0.003	0.110 ± 0.003

*$t_{1/2}$ for Ce^{144} = 270 days.

**Neutron absorption of Nd^{143} was not sufficient to change Nd^{145} and Nd^{144} fission yields.

isotopes of zirconium for natural contamination. The mass spectrometric ration together with the relative yields are shown in Table XLIII.

(c) Molybdenum

The relative fission yields of Mo^{97}, Mo^{98} and Mo^{100} determined from sample D along with the observed mass spectrometric ratios are shown in Table XLIV. The yield of Mo^{95} was not estimated from this sample. The relative yields of those isotopes measured in this work have been given in Table XLV together with the literature values. Where more than one determination of a yield was carried out, the value quoted in the following table represents an average weighted according to the inverse square of the standard deviations.

(I) The Absolute Yields of the Light Mass Fragments in the Thermal Neutron Fission of U^{235}

Absolute fission yields were obtained from the relative yields shown in Table XLV in the following manner. The relative strontium yields were normalized to those of zirconium by means of the relative yields of Y^{89} and Y^{91}. In the same manner, the molybdenum yields were normalized to those of zirconium at mass 95 using the ratio of mass 95 to mass 100 reported by Steinberg et al. (2).

Since no absolute yield was measured for any of these nuclides, they have been normalized to the 3.57% yield for Sr^{88} given by Katcoff (17). This value is the average of values 3.53% obtained by Petruska et al. (13) and 3.61% found by Glendenin et al. (3). The final results along with those obtained from the literature are shown in Table XLVI.

TABLE XLIII

Relative Yields of the Zirconium Isotopes in the Thermal Neutron Fission of U^{235}

Sample	Time From End of Irradiation (days)	Isotope	Mass Spectrometric Ratio	Ratio Corrected For Contamination	Ratio Corrected For Decay
A		90	0.0299	-	-
		91	-	-	-
		92	0.940 ± 0.021	0.9305 ± 0.021	0.9305 ± 0.021
		93	1.000	1.000	1.000
		94	1.011 ± 0.016	1.001 ± 0.016	1.001 ± 0.016
	66.1	95	0.4446 ± 0.0080	0.4446 ± 0.0080	1.007 ± 0.002
		96	0.9624 ± 0.0016	0.9208 ± 0.0016	0.9608 ± 0.0016
D		90	0.0466*	-	-
	135.5	91	0.854 ± 0.012	0.8467 ± 0.012	0.917 ± 0.013
		92	0.936 ± 0.014	0.926 ± 0.014	0.926 ± 0.014
		93	1.000	1.000	1.000
		94	1.020 ± 0.014	1.010 ± 0.014	1.010 ± 0.014
	151.5	95	-	-	-
		96	0.991 ± 0.015	0.989 ± 0.015	0.989 ± 0.015

*Mass 90 yield consists of a 0.0158 contribution from the decay of Sr^{90} and hence only 0.0308 from natural zirconium.

TABLE XLIV

Relative Yields of the Molybdenum Isotopes in the Thermal Neutron Fission of U^{235}

Sample	Time From End of Irradiation (days)	Isotope	Mass Spectrometric Ratio	Corrected For Contamination
D	97.5	95	-	"
		96	0.1504	-
		97	1.052 ± 0.02	0.961 ± 0.12
		98	1.129	0.910 ± 0.016
		100	1.092	1.00

TABLE XIV

Relative Yields of the Measured Nuclides From U^{235} Fission Together With Literature Values

	Relative Yield		
Isotope	This Work	Petruska (15)	Katcoff (17)
Sr^{86}	0.622 ± 0.015	0.6150	0.6187
Sr^{89}	0.8013 ± 0.0094	-	0.8204
Sr^{90}	1.000	1.000	1.000
Y^{89}	1.000		
Y^{91}	1.200 ± 0.012		
Zr^{91}	0.917 ± 0.013		0.905
Zr^{92}	0.927 ± 0.013		0.935
Zr^{93}	1.000		1.00
Zr^{94}	1.006 ± 0.015		0.994
Zr^{95}	1.007 ± 0.002		-
Zr^{96}	0.985 ± 0.015		0.982
Mo^{95}	-		0.995
Mo^{97}	0.961 ± 0.012		0.966
Mo^{98}	0.901 ± 0.016		0.917
Mo^{100}	1.000		1.000
Nd^{145}	1.000	1.000	1.000
Nd^{144}	0.928 ± 0.023	0.930	0.948
Nd^{145}	0.667 ± 0.010	0.665	0.661
Nd^{146}	0.5040 ± 0.0097	0.505	0.513
Nd^{148}	0.281 ± 0.002	0.281	0.284
Nd^{150}	0.110 ± 0.003	0.110	0.112

TABLE XLVI

Absolute Yields of the Light Fragments in the Thermal Neutron Fission of U^{235}

Mass Chain	Element	Percent Yield This Work	Percent Yield Katcoff (17)
72 - 80			0.177
81	Se		0.14
82			0.26
83	Kr		0.545
84	Kr		1.00
85	Rb (Kr)		1.30
86	Kr		2.02
87	Rb		2.49
88	Sr	3.57	3.57
89	Sr (Y)	4.60	4.78
90	Sr	5.74	5.77
91	Zr (Y)	5.79	5.84
92	Zr	5.86	6.03
93	Zr	6.32	6.45
94	Zr	6.34	6.40
95	Zr (Mo)	6.36	6.27
96	Zr	6.25	6.33
97	Mo	6.15	6.09
98	Mo	5.76	5.78
99			6.06
100	Mo	6.40	6.30
101	Ru		5.00
102	Ru		4.10
103			3.00
104	Ru		1.80
105			0.9
106	Ru		0.38
107 - 117			0.414
		TOTAL	99.20%

DISCUSSION

(A) Thermal Neutron Absorption Cross Section

(a) Xenon-135

The precision of the values obtained for the effective neutron absorption cross section of Xe^{135} shown in Table V includes only the standard deviation of the observations carried out in this work.

No estimate of the absolute accuracy of the values is possible without including the accuracy of the 36.5 barn value used for the 2200m/sec. absorption cross section of the Co^{59} and the 9.20 hour half-life used for Xe^{135}. To a lesser extent values given in Table XI would depend on the accuracy of other quantities such as the resonance integral for Co^{59} and the half-life of I^{135}. The precision of the cross sections obtained from the samples in assembly B are not as good as those from assembly C. This arises from the relatively smaller amount of capture by the Xe^{135} at the lower flux rather than from the precision of the measurements.

Previous values of the effective absorption cross section of Xe^{135} have been made by essentially the same method as in this work. Ivanov et al. (21) have found a value of 3.2 ± 1.0 megabarns and Petruska et al. (15) 3.47 megabarns. Direct comparison of these with each other or with the values given in Table XI is difficult as neutron temperatures were not measured. The precision of the 3.47 megabarn value obtained by Petruska

et al. was difficult to estimate in view of flux variations during the irradiation, a factor which was not inherent in the present work. Although the neutron temperature was not determined by Petruska et al., the irradiation position in the NRX reactor for this sample was similar to that of assembly B. If the neutron temperature at the time of this irradiation was essentially the same as for the irradiation in the present work, the agreement of the values is very good.

The total cross section measurements of E. C. Smith (19) and S. Bernstein (18) have been used by Westcott (20) to evaluate the effective neutron absorption cross section of Xe^{135} at various temperatures. The calculated values for temperatures corresponding to this work are given in Table XLVII.

These values are not strictly comparable with those obtained in this work since they represent the effective absorption for a pure Maxwellian spectrum of neutrons. The contribution of absorption by epithermal neutrons cannot be estimated until the resonance integral for Xe^{135} is known. The values comparable with this work would be slightly less than those given in Table XLVII, the greater reduction applying to the 120° values for which the epithermal flux is greater. Comparison of the possible values for the effective cross section of Xe^{135} given in Table XLVII with the values obtained in this work given in Table XI suggests however that the values calculated from the data of Bernstein with the statistical weight factor of $g = 5/8$ are most consistent with the present work.

(b) Samarium-149

The effective neutron absorption cross section of Sm^{149} is strongly

TABLE XLVII

Effective Absorption Cross Sections of Xe^{135} Calculated From Total Cross Sections

	$\sigma_{Xe^{135}}$ ($g = 3/8$) x 10^5 Barns		$\sigma_{Xe^{135}}$ ($g = 5/8$) x 10^5 Barns	
	120°C	137°C	120°C	137°C
Smith	29.78	29.96	33.78	33.98
Bernstein	26.95	27.12	30.19	30.45

dependent on the neutron temperature since there is a strong resonance at 0.09 ev (24). The value of σ_o calculated from the effective cross sections should of course be a constant. The excellent agreement of the values 42,600 and 42,500 barns obtained for σ_o from samples B and C (experimental results, section B) is an indication of the self-consistency of the data used in their calculation. Rose et al. (50) independently reported values for the 2200m/sec. cross section of Sm^{149} at the same time as the present values were published (35). Using the pile oscillator technique to obtain effective cross sections and the Tables of Westcott for values of g and s, they have found a value of 42,100 ± 700 barns using equation (2), Appendix A. This confirmation of the present work would indicate that the previously accepted value of 39,700 barns (24) for the Sm^{149} cross section for 2200m/sec. neutrons is low.

(B) Relative and Absolute Yields of Heavy Mass Fragments in the Thermal Neutron Fission of Pu^{239}

The accuracy of the relative yields of the isotopes of a given element depends on the accuracy of the directly determined mass spectrometric measurements whereas the fission yields also depend on isotope dilution measurements.

The precision of the relative yields of the heavy mass fragments given in Tables XV, XVII, XVIII and XIX in each case are better than 1% and agree within these limits with the values previously published (3) and (4) except at three mass regions. The most serious difference is the ratio of $\frac{Cs^{133}}{Cs^{137}}$ shown in Table XV. Since Cs^{133} is the stable isotope which occurs in nature it may be considered that high values of this ratio are the result of stable contamination. In the previous determination from

this laboratory, column 7, Table XV, only partial recovery of the fission products was achieved. Recent unpublished work in this laboratory has established that the mobility of the 5-day Xe^{133} precursor to Cs^{133} can materially alter fission yield ratios of cesium isotopes in oxide samples. The value obtained by Krishanski et al. (4) can not be assessed without further information, but the new value presented in Table XV has been confirmed with measurements from several entirely different irradiations. A similar type of variation but to a lesser extent has also been observed at mass 140 (see Table XIA) which apparently does not depend on stable contamination.

A further difference is observed at masses 152 and 154 (see Table XVII). The yields given by Krishanski et al. (4) were corrected assuming Sm^{148} is contamination arising from the presence of natural samarium. In fact the Sm^{148} was probably produced by decay of Pm^{148} formed by an (n, γ) reaction with Pm^{147} and hence this correction should not have been made. The values of Krishanski et al. (4) without correction for Sm^{148} correspond closely to the values obtained in this work.

Fritze and coworkers in their simultaneous determinations of xenon and krypton from the same Pu-Al alloy sample obtain a cumulative fission yield of 3.79 ± 0.11 for Xe^{131}. This is in good agreement with the value of 3.77 obtained in this work from the measured yield of Cs^{133} and the relative yields of Xe^{133} and Xe^{131} previously given by Fleming and Thode (38).

The final values of the cumulative fission yields of Pu^{239} given in Table XXVII have been normalised so that the yields total 100%. The

values given in Table XXV depend on the calculation of the total number of fissions occurring in each sample. In the case of the PuO_2 sample where the neutron temperature was not measured (hence the fission cross section doubtful) and where the self-shielding correction amounted to about 40%, it is considered fortuitous that the yields shown in Table XXV total 100.8%. For this sample, the values given in Table XXVII are therefore to be preferred. In the case of the Pu-Al alloy sample these factors were more carefully controlled and therefore the 99.1% summation of the yields in Table XXV could well be a measure o the cumulative errors in the several determinations or in the values of the few yields which have been assumed. The final values for this sample shown in Table XXVII have nevertheless been normalized to 100% since they are then independent of the calculated number of fissions, a factor which is dependent on the relative cross section of Pu^{239} and Co^{59} and the self-shielding correction. The agreement with the yields shown in Table XXIV are taken as a measure of the absence of loss or fractionation of fission products from the sample.

The yields of Wilson et al. (3) also shown in Table XXVII are now assumed to be in error from fractionation which occurred in the partial extraction of the fission products from the PuO_2. The radiochemical yields summarized by Steinberg et al. (2) are difficult to compare with the present values since their summation is only 93%.

The values of the yields obtained from the two independent determinations shown in columns 2 and 3 of Table XXVII agree to better than 2% at most masses and the average values shown in column 4 of Table XXVII are considered to have an absolute accuracy of better than 3% at each mass.

(C) Relative and Absolute Yields of the Light Mass Fragments in the Thermal Neutron Fission of Pu^{239} and U^{235}

The precision of most of the relative yields obtained for the light mass fragments, both for Pu^{239} and U^{235} fission shows a marked decrease over those for the heavy mass fragments. Such factors as the presence of natural molybdenum in the tungsten filament which required a 10-15% correction to be made to the observed mass spectrum reduced the precision of the relative yields. Despite of such factors, however, precisions between 1 and 2% have been obtained in most cases.

Difficulties arise in attempting to obtain a complete equilibration between the small quantities of zirconium in an irradiated sample and an isotope diluent because of absorption characteristics of this element. Therefore, the zirconium in the Pu^{239} and U^{235} samples was not isotope diluted but normalized to the other elements through the molybdenum and strontium respectively.

The absolute yields of the light mass fragments from Pu^{239} shown in Table XXXIX were obtained from the relative yields by normalization to the 6.9% yield of Cs^{133} which was obtained above as an absolute yield. This method related the yields of the light mass fragments directly to to those of the heavy mass fragments without relying on the estimation of the number of fissions.

The relative yields of only twelve of the light mass fission fragments (i.e. isotopes of Sr, I, Zr and Mo) were determined from U^{235} fission products. The absolute yields were obtained by normalization to the strontium using 3.57% for the absolute yield of Sr^{88} which represents an average of the values 3.53 and 3.61 reported by Steinberg et al. (2) and Petruska et al. (13) respectively.

To date, values for the absolute yields of the light mass fragments from Pu^{239} fission consists of only a few radiochemical yields summarized by Katcoff (17) and the mass spectrometric yields of the krypton isotopes determined by Fritze et al. (16) in subsequent determinations.

These values for the krypton isotopes are essentially the same as the values reported in this thesis when the Kr^{85} is recalculated using a 0.299 branching ratio.

The absolute yields for the thermal neutron fission of U^{235} are in general within 2% of the values reported here, however the yields of masses 89 and 91 differ by about 4% and 3% respectively.

The percent yields of the light mass fragments of Pu^{239} shown in Table XXXIX total 100.13% which assures confidence in the quoted absolute yields. 98.71% is obtained for U^{235} from the values in column 3. Table XLVI together with literature values shown in column 4. This may be considered satisfactory since not only was the accuracy of the relative yields less than for the heavy mass fragments, but a larger number of yields had to be obtained from the literature.

The accuracy of the relative fission yields for the light mass fragments for both U^{235} and Pu^{239} was 1-2%. The values of the absolute yields shown in Tables XXXIX and XLVI are considered to have an accuracy of 3-4%.

(b) Interpretation of the Fission Yields of Fragments Formed in the Thermal Neutron Fission of Pu^{239} and U^{235}

The complete mass vs. fission yield curve has been plotted in Figure 3 showing the predominant fine structure in both mass regions in the thermal neutron fission of Pu^{239}.

In order to assess the experimental fission yields, it is convenient to fold the fission yield curves over each other as shown in Figure 4. Since the sum of the mass numbers of corresponding fission fragments together with the number of emitted neutrons must be 240 (Pu^{239} + 1 neutron), it is necessary to decide which masses should be made to correspond. In Figure 4, the cumulative yield of each light mass chain has been plotted over that of a heavy mass chain in such a manner that the sums of their masses total 237.

Experimentally it may be seen from Figure 4 that the cumulative yield of each measured fission chain from mass 138-154 corresponds to the cumulative yield of a measured light mass chain from 83-99. For example the yield of mass 90 is equal to the yield of mass 147.

Since β decay does not change the mass number of the members of a β-decay chain, any explanation of the origin of the cumulative yields need not be concerned with the charge distribution of complementary fragments. Thus, if three neutrons are emitted in every fission, whenever a mass 90 fragment is formed there must be a corresponding fragment of mass 147 and the yields of masses 90 and 147 will be equal.

The question arises as to whether the equivalence of the yields of masses 90 and 147 could have resulted from two neutron emission for half the fission events and four in the other half, or any other modes of division which could average three. It appears that such a possibility can only occur for the conditions that all cumulative yields are equal, an obvious contradiction of experimental observation. This, however, has not been proved. It may well be that the experimental data is sufficient to prove that not only are three neutrons emitted per fission

but also that exactly three are emitted in every fission.

Although there are not many yields measured in this work which are in the mass region 106-118 and 118-131, it appears that these yields would correspond if plotted so that rather than the 237 as shown in Figure 4, the sums of corresponding masses would total between 237.5 and 238. It is evident from Figure 4 that the yields in the region of mass 105-99 do not correspond to the yields in mass region 132-138. Part of this lack of correspondence may result from delayed neutron emission by I^{137}. It may be seen that an increase in yield at mass 137 and decrease in yield at mass 136 would lead to a better correspondence with the yields of masses 100 and 99 respectively. It is doubtful, however, if all of the observed difference may be attributed to the delayed neutron emission by I^{137}. This would require 0.005 delayed neutrons per fission for I^{137} whereas only 0.0018 neutrons have been attributed to this nuclide by Keepin et al. (51). It is apparent that part of the difference in yield of masses 101 and 136 must be formed in a different manner as will be discussed below.

Keepin et al. (51) and Stehney et al. (52) have also shown that approximately equal amounts of delayed neutron emission occurs from I^{138} and I^{139}. The yield of this 139 mass chain has not been measured but it may fall considerably below that of mass 98. The measured yield of mass 138 has probably gained through delayed neutron emission by I^{139} as much as it has lost from delayed neutron emission by I^{138} and it is therefore not significantly displaced from a smooth mass-yield curve.

There is still however a large difference in yield between the light mass fragments between masses 105 and 101 and heavy mass fragments between masses 132 and 136 which must be explained in some other manner.

Since there are three neutrons emitted per fission to the right of this region as shown in Figure 4 and about two neutrons per fission to the left of this region it is apparent that there must be a change in the neutron emission characteristics in either the light or heavy fragments leading to these cumulative yields. One possibility is that an increased stability of primary fragments in the heavy mass region, possibly those having either 82 neutrons or 50 protons, may minimize the probability of neutron emission from these fragments, which would cause the cumulative yields of the heavy mass fragments to be greater than those of the corresponding light mass fragments. This may be clarified from the following considerations. Since the heavy mass distribution is not as wide as that of the light, the reduction in width would result in an increased cumulative yield in the mass region where the reductions in neutron emission occurred. This possibility is consistent with the Fraser and Milton (53) observation that the relative neutron emission probability in the heavy fragments is considerably less than that for the light when the ratio of heavy mass to light mass is about 1.3 (for U^{233} fission). It will be noted that without this data of Fraser and Milton it would be equally possible from the present data to consider the light mass distribution wider than that of the heavy mass yield distribution as a result of increase in neutron yield in the mass region 101-106. This would lower the yields of the light mass cumulative yields in comparison with those of the heavy mass fragments.

An important consequence of the complete mass yield curve is that it is possible to obtain the total number of neutrons released in the thermal neutron fission of Pu^{239} from the relation $\bar{\nu} = 240 - 2\frac{\Sigma(\text{mass} \times \text{yield})}{\Sigma \text{yield}}$

A value of 2.80 ± 0.08 taking the accuracy of ± 3% for the measured fission yields. This is in essential agreement with the world-consistent value of 2.90 ± 0.04 given by Hughes (50).

Figure 5 shows the comparison between the light and heavy mass-yield distribution for U^{235}.

The yields of the heavy mass fission products are taken from Petruska et al. (13) and those of the light mass fragments are taken from Katcoff's summary of yields (17) given in Table XLVI except for those in the mass region 88-100 which were measured in this work and given in Table XLVI.

It may be noted that the right side of Figure 5 indicates an excellent correspondence between the forms of the light and heavy mass yield curves in the same region as the correspondence occurred for Pu^{239}. The correspondence occurs however for the average neutron emission of 2.5 neutrons per fission for these mass regions. Also the yield of a given light mass chain does not correspond to the yield of a heavy mass chain as it did in the case of Pu^{239}. It is found that the cumulative yields of the light mass fragments are intermediate to the cumulative yields of heavy mass fission products. Since 2.5 neutrons can not be emitted in any fission it may be assumed that in these mass regions two neutrons are emitted in one half the fissions and in the other half three neutrons are emitted. i. e., in the formation of mass 88, mass 145 is produced if 3 neutrons are emitted and mass 146 if 2 neutrons are emitted. Since the average number of neutrons for these mass regions is 2.5 the relative amount of mass 90 should be intermediate to those of masses 145 and 146. This is consistent with observation but the explanation

presented is subject to the same limitations as considered above with respect to Pu^{239} fission yields.

The left side of Figure 5 indicates an equivalence of each fission yield of a light mass fragment with one of the heavy mass yields. The curves would also correspondwhen equivalent yields add to 234 (2 neutron emission).

The poor correspondence between the light and heavy mass yields in the mass region where the fine structure occurs is evidently similar to that found in Pu^{239} fission.

The value of $\bar{\nu}$ estimated from the relation $\bar{\nu} = 236 - \frac{2\Sigma \text{ mass} \times \text{yield}}{\Sigma \text{ yield}}$ is 2.20 ± 0.07, the error being based on accuracy of $\pm$ 3% for the fission yields (13). The "world-consistent" value of $\bar{\nu}$ given by Hughes (24) is 2.47 ± 0.03.

It is of some interest to compare the light mass-yield curve fol U^{235} with that for Pu^{239} as shown in Figure 6. This shows the large displacement of the Pu^{239} yields towards heavier masses, an observation which is commonly known (1). Attention may also be drawn to the observation that the yield of mass 100 is favoured in both Pu^{239} and U^{235} thermal neutron fission.

In U^{235} fission it had been commonly considered that this yield was the complement of a favoured yield at mass 134, but this is not the case for Pu^{239} fission where it is the complement of mass 137. As there is no major neutron or proton shell associated with the primary fragments that might lead to this mass yield, there is suggested reason for its high value.

Another observation related to Figure 6 is that yields of 85 and 87 are low in relation to a smooth curve for both Pu^{239} and U^{235}. It is suggested that this effect is related to delayed neutron emission as previously suggested by Tetsuoka et al. (13). It is apparent that the relatively higher delayed neutron yields for uranium fission (0.015 for U^{235} compared to 0.0061 neutrons/fission from Pu^{239} (51)) are largely dependent on the higher cumulative yields in this mass region for U^{235}.

Figure 7 shows the relation between the yields of the heavy mass fragments from U^{235} and Pu^{239}. It appears that the Pu^{239} yields are displaced to a lower mass than those of U^{235}, a fact not generally recognised from previous work.

BIBLIOGRAPHY

1. Steinberg, E. P. and Freedman, M. S.: National Nuclear Energy Series, Ser. 9, Div. IV (McGraw-Hill Book Company Inc., New York, 1951). Paper 219.

2. Steinberg, E. P. and Glendenin, L. E.: 1st International Conference on the Peaceful Uses of Atomic Energy, Vol. 7, Paper 614, 3-14 (1955).

3. Miles, B. M., Petruska, J. A. and Tomlinson, R. H.: Can. J. Chem. 34: 227-232 (1956).

4. Krishansky, L. P., Raly, Ya, Surin, A. M. and Predvoshensky, B. K: Soviet J. Atomic Energy 2, 334 (1957).

5. Coryell, C. D. and Sugarman, L.: Radiochemical Series: The Fission Products (McGraw-Hill Book Company Inc., New York 1951), National Nuclear Energy Series, Ser. 9, Div. IV, Papers 1-11.

6. Engelkemeir, D. W., Freedman, M. S., Seiler, J. A., Steinberg, E. P. and Winsberg, L.: National Nuclear Energy Series, Ser. 9, Div. IV, Paper 201 (1951).

7. Freedman, M. S. and Steinberg, E. P.: National Nuclear Energy Series, Ser. 9, Div. IV, Paper 202 (1951).

8. Freedman, M. S. and Steinberg, E. P.: National Nuclear Energy Series, Ser. 9, Div. IV, Paper 200 (1951).

9. Engelkemeir, D. W., Seiler, J. A., Steinberg, E. P. and Winsberg, L.: National Nuclear Energy Series, Ser. 9, Div. IV, Paper 4 (1951).

10. Engelkemeir, D. W., Seiler, J. A., Steinberg, E. P., Winsberg, L. and Povey, T. S.: National Nuclear Energy Series, Ser. 9, Div. IV, Paper 5 (1951).

11. Bartholomew, R. F., Brown, F., Hawkings, R. C., Merritt, W. F., and Yaffe, L.: Can. J. Chem. 31, 120 (1953).

12. Yaffe, L., Rhode, E. O., Merritt, W. F., Hawkings, R. C., Brown, F., and Bartholomew, R. F.: Can. J. Chem. 32, 1017 (1954).

13. Petruska, J. A., Rhode, E. O. and Tomlinson, R. H.: Can. J. Phys. 33, 693-706 (1955).

14. Petruska, J. A., Melaika, E. A. and Tomlinson, R. H.: Can. J. Phys. 33, 640-649 (1955).

15. Kukavadze, G. M., Anikina, M. P., Goldin, L. L. and Ershler, B. V.: Conf. of the Academy of Sciences of the U.S.S.R. on the Peaceful Uses of Atomic Energy, English Translation, 125 (1955).

16. Fritze, K., McMullen, C. C. and Thode, H. G.: 2nd International Conference on the Peaceful Uses of Atomic Energy, Paper 187 (1958).

17. Katcoff, S.: Nucleonics Vol. 16, No. 4, 78-85, April (1958).

18. Bernstein, S.: Phys. Rev. 102, No. 3, 823 (1956).

19. Smith, E. C., Desmuke, N. and Atta, Mrs.: (unpublished).

20. Westcott, C. H.: "Effective Cross Section Values for Well-Moderated Thermal Reactor Spectra" A.E.C.L. Report 670 (1958).

21. Ivanov, R. N., Gorshkov, V. K., Anikina, M. P. Kukavdze, G. M. and Ershler, B. V.: The Soviet J. of Atomic Energy, Vol. 3, No. 12, 1436 (1957).

22. Inghram, M. G., Hayden, R. J. and Hess, D. C.: Phys. Rev., 72, 271-274 (1950).

23. Aitkens, K. L., Littler, D. J., Lockett, E. B. and Palmer, G. H.: J. Nuclear Energy, 4, 33, 1957.

24. Hughes, D. J. and Harvey, J. A.: Neutron Cross Sections, Brookhaven National Laboratories, Report BNL-325 (Upton, New York, 1955).

25. Irish, D. B.: M.Sc. Thesis, McMaster University, September, 1956.

26. Inghram, M. G. and Chupka, W. A.: Surface Ionization Using Multiple Filaments, Rev. Sci. Instr., 24, No. 7: 518-520 (1953).

27. Petruska, J. A.: M.Sc. Thesis, McMaster University, September, 1954.

28. Schubert, J. and Conn, E. E.: Nucleonics, Vol. 4, page 2: January-June, 1949.

29. Parker, M. J.: M. Sc. Thesis, McMaster University, September, 1953.

30. Hume, D. N.: National Nuclear Energy Series, Ser. 9, Div. IV, Paper 261 (1951).

31. Glendenin, L. E.: National Nuclear Energy Series, Ser. 9, Div. IV, Paper 258 (1951).

32. Nier, A. O.: Phys. Rev. 79, 450 (1950).

33. Bigham, C. B.: "Thermal Neutron Temperature in NRX Self-Serve Positions S-3-5 and S-6-3" A.E.C.L. Report C.R.R.P., 765, 1958.

34. Wiles, D. M. and Tomlinson, R. H.: Phys. Rev. 99, 188 (1955).

35. Bidinosti, D. R., Fickel, H. R. and Tomlinson, R. H.: 2nd International Conference on the Peaceful Uses of Atomic Energy, Paper 201 (1958).

36. Melaika, E. A., Parker, M. J., Petrunka, J. A. and Tomlinson, R. H.: Can. J. Chem. 33, 830 (1955).

37. Walker, W. H. and Thode, H. G.: Phys. Rev. 90, 448 (1953).

38. Fleming, W. H. and Thode, H. G.: Can. J. Chem. 34, 193 (1956).

39. Jervis, R. F.: Private Communication, Atomic Energy of Canada Ltd., Chalk River, Canada (1958).

40. Bergstrom, I. M. Siegbahn Commemorative, Volume XX, Uppsala 307 (1951).

41. Wiles, D. M. and Tomlinson, R. H.: Can. J. Phys. 33, 133 (1955).

42. Kahn, B. and Lyon, W. S.: Phys. Rev. 98, 58 (1955).

43. Herrmann, G. and Straussman, F.: Z. Naturforsch, 11a, 946 (1956).

44. Engelkemeir, D. W., Brady, E. L. and Steinberg, E. P.: NNES-PPR 9, 722 (1951).

45. Cork, J. M., LeBlanc, J. M., Martin, D. W., Nester, W. H. and Brice, M. K.: Phys. Rev. 90, 579 (1953).

46. Wright, H. W., Wyatt, E. I., Reynolds, S. A., Lyon, W. S. and Handley, T. H.: Nuclear Sci. Eng. 2, 157 (1957).

47. Schuman, R. P., Jones, M. E. and Newherter, A. C.: J. Inorg. Nuclear Chem. 3, 160 (1956).

48. Merritt, W. F., Campion, P. J. and Hawkings, R. C.: Can. J. Phys. 35, 16 (1957).

49. Manless, R. K. and Thode, H. G.: Can. J. Phys. 33, 541 (1955).

50. Rose, H., Cooper, W. A. and Taltersall, R. B.: 2nd International Conference on the Peaceful Uses of Atomic Energy, Paper 14 (1958).

51. Keepin, G. R. Wimmett, T. F. and Zeigler, R. K.: J. Nuclear Energy 6, 1-21 (1957).

52. Stehney, A. F. and Perlow, G. J.: 2nd International Conference on the Peaceful Uses of Atomic Energy, Paper 691 (1958).

53. Fraser, J. S. and Milton, J. C. D.: Phys. Rev. 93, 818 (1954).

APPENDIX

(A) Equations Involved in the Determination of Flux and Effective Cross Section

The integrated flux is related to the disintegration rate of Co^{60} with equation (1):

$$\phi t = -\frac{dN_{60}}{dt} \times \frac{1}{\lambda N_{59} \hat{\sigma}_{Co} S_{Co}} \qquad (1)$$

where λ = the decay constant for Co^{60} = 4.18×10^{-9} sec^{-1}.

N_{59} = number of atoms of cobalt-59.

$\hat{\sigma}_{Co}$ = effective cross section for cobalt in cm^2.

S_{Co} = the flux self-shielding correction for cobalt wire (14).

The effective cross section required in equation (1) may be calculated from the 2200m/sec. cross section with equation (2):

$$\hat{\sigma} = \sigma_o(g + rs) \qquad (2)$$

where σ_o = the 2200m/sec. cross section.

g represents the departure of the nuclide's cross section from a $\frac{1}{v}$ law in terms of its effect for a Maxwellian neutron spectrum.

r = epithermal index as defined by Westcott (20).

s characterizes the departure of the nuclide's cross section from a $\frac{1}{v}$ law in the epithermal region.

The effective cross section of Sm^{149} ($\hat{\sigma}_{Sm149}$) may be obtained in an irradiated sample of samarium by measuring the change in the $\frac{Sm^{150}}{Sm^{149}}$

resulting from the neutron absorption and substituting in equation (3):

$$\frac{Sm^{150}}{Sm^{149}} = 1.54\ (_e\hat{\sigma}_{Sm149}\ \phi t) - 1 \qquad (3)$$

where 1.54 = the natural ratio of $\frac{Sm^{149}}{Sm^{150}}$ in the unirradiated sample.

$\frac{Sm^{150}}{Sm^{149}}$ = the observed ratio after irradiation.

(B) Relation Between $\frac{Cs^{135}}{Y^{135}}$ Ratio and $_{54}\sigma^{135}\ \phi$

The ratio of the number of atoms of Cs^{135} found after a neutron irradiation of U^{235} to the total number of atoms of mass 135 produced was determined by solution of the following differential equations:

$$\frac{dU^{235}}{dt} = U^{235}\ {}_{92}\sigma_a^{235}\ \phi$$

$$\frac{dI^{135}}{dt} = 0.95\ U^{235}\ {}_{92}\sigma_f^{235}\ \phi\ y^{135} - I^{135}\ {}_{53}\lambda^{135}$$

$$\frac{dXe^{135}}{dt} = I^{135}\ {}_{53}\lambda^{135} - Xe^{135}\left({}_{54}\lambda^{135} + {}_{54}\sigma^{135}\ \phi\right) + 0.05\ U^{235}\ {}_{92}\sigma_f^{235}\ \phi\ y^{135}$$

$$\frac{dCs^{135}}{dt} = Xe^{135}\ {}_{54}\lambda^{135}$$

and where y^{135} is the percent cumulative yield of mass 135 chain, ϕ is the 2200m/sec. neutron flux, σ and λ, are the effective neutron cross section and decay constant for the nuclides indicated by the appropriate subscripts and superscripts.

In these equations it is assumed that there is a 5% primary yield of Xe^{135} which is the amount estimated from the Glendenin hypothesis of equal charge displacement (2). It is also assumed that the remaining 95%

of this mass chain is produced directly as I^{135} since the half-lives of the precursors are short compared to the irradiation times for which solutions to these equations are required. Equation (4) may be derived from these differential equations for the conditions that all the I^{135} and Xe^{135} present at the end of the irradiation have decayed to Cs^{135} and that there is a negligible depletion of U^{235} during the irradiation.

$$\frac{Cs^{135}}{Y^{135}} = \frac{{}_{54}\lambda^{135}}{K} - \frac{\sigma\phi}{t}\left[\frac{e^{-Kt}-1}{K^2} + \frac{0.95\left(e^{-{}_{53}\lambda^{135}t}-1\right)}{{}_{53}\lambda^{135}\left(K-{}_{53}\lambda^{135}\right)} - \frac{0.95\left(e^{-Kt}-1\right)}{K\left(K-{}_{53}\lambda^{135}\right)}\right] \quad (4)$$

where Y^{135} is total number of atoms of mass 135 produced, and K is equal to:

$$ {}_{54}\lambda^{135} + {}_{54}\sigma^{135}\phi \, .$$

The values of ${}_{54}\sigma^{135}\phi$ shown in Table IX have been calculated from the ratios of $\frac{Cs^{135}}{Y^{135}}$ using equation (4) with values of ${}_{53}\lambda^{135} = .1034$ hr , ${}_{54}\lambda^{135} = 0.752$ hr^{-1} and t = 87.83 hours.

(C) Determination of Cumulative Yield of Cs^{135} in Pu^{239} Fission

The cumulative yield of Cs^{135} in the thermal neutron fission of Pu^{239} may be determined substituting the appropriate values from Table XVI into equation (4), Appendix B.

For the samples G and H, the irradiation was not continuous due to reactor shut-downs during the period that the samples were in the reactor. The times of irradiation for these samples could be divided into four and five periods as shown in Table XVI, the time between each periods being long enough to allow essentially all of the Xe^{135} formed during the previous irradiation to decay before the next irradiation commenced.

The ratios of the measured Cs^{135} to the yield of mass 135 by averaging the values listed in Table XVI for the continuous irradiation periods, weighting each according to the fraction of the total irradiation time which it involves.

(b) The decay equation for the transformation $Pm^{147} \rightarrow Sm^{147}$

(i) The cumulative yield of Sm^{147} can be calculated from yield measured at any time t_2 after the irradiation by application of the following approximate equations which neglects the Nd^{147} precursor in this decay chain.

$$\frac{Y_{149}}{Y_{147}} = \frac{N^{149}}{N^{147}} \left[1 - \left\{ \frac{1}{\lambda t_1} \left(1 - e^{-\lambda t_1} \right) e^{-\lambda t_2} \right\} \right] \qquad (5)$$

where Y represents the cumulative yield of the samarium isotope designated by the subscript.

N represents the measured value of the yield of the samarium isotope designated by the subscript.

t_1 = time of irradiation (31.19 days for sample).

t_2 = time of analysis after irradiation (362.42 days).

λ = decay constant = $\frac{.693}{t_{\frac{1}{2}}} = \frac{.693}{919.8}$ d^{-1}.

(ii) The correction to the Sm^{151} and Sm^{152} due to the reaction Sm^{151} (n, γ) Sm^{152}.

The measured $\frac{Sm^{151}}{Sm^{152}}$ ratio depends on the product of flux and time of irradiation.

For the cumulative fission yields of these isotopes the measured ratio must be corrected according to the following relationship:

TABLE XVI

Irradiation Times and Ratios of Cs^{135}/Y^{135}

	H		I	
	Irradiation Period (hours)	R^{135}/Y^{135}	Irradiation Period (hours)	R^{135}/Y^{135}
#1	5.384	0.7162	-	-
#2	105.8	0.7589	105.8	0.7549
#3	224.8	0.7519	224.8	0.7581
#4	73.69	0.7621	73.69	0.7776
#5	75.55	0.7803	75.55	0.7758

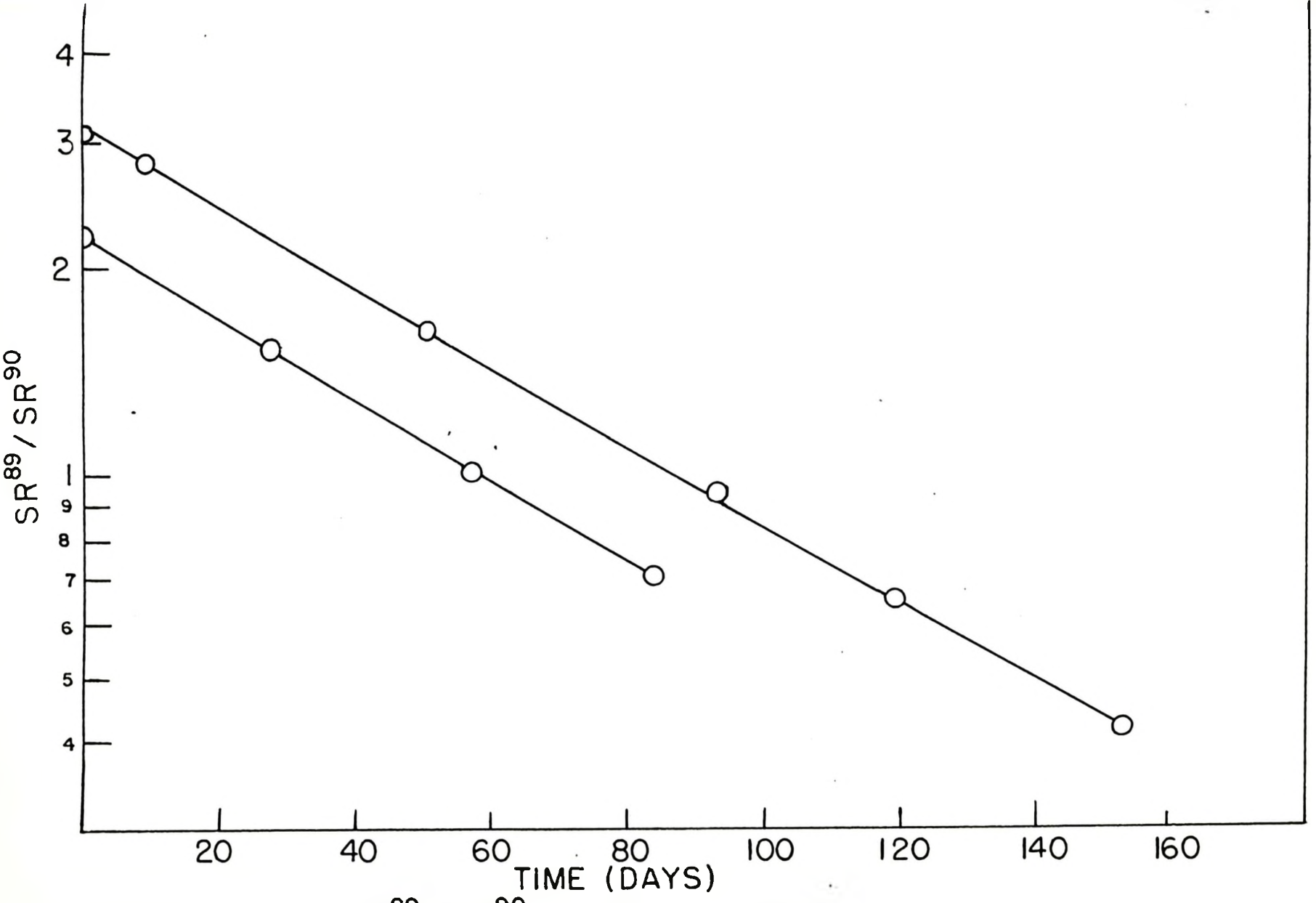

FIGURE 1 SR^{89}/SR^{90} VS TIME

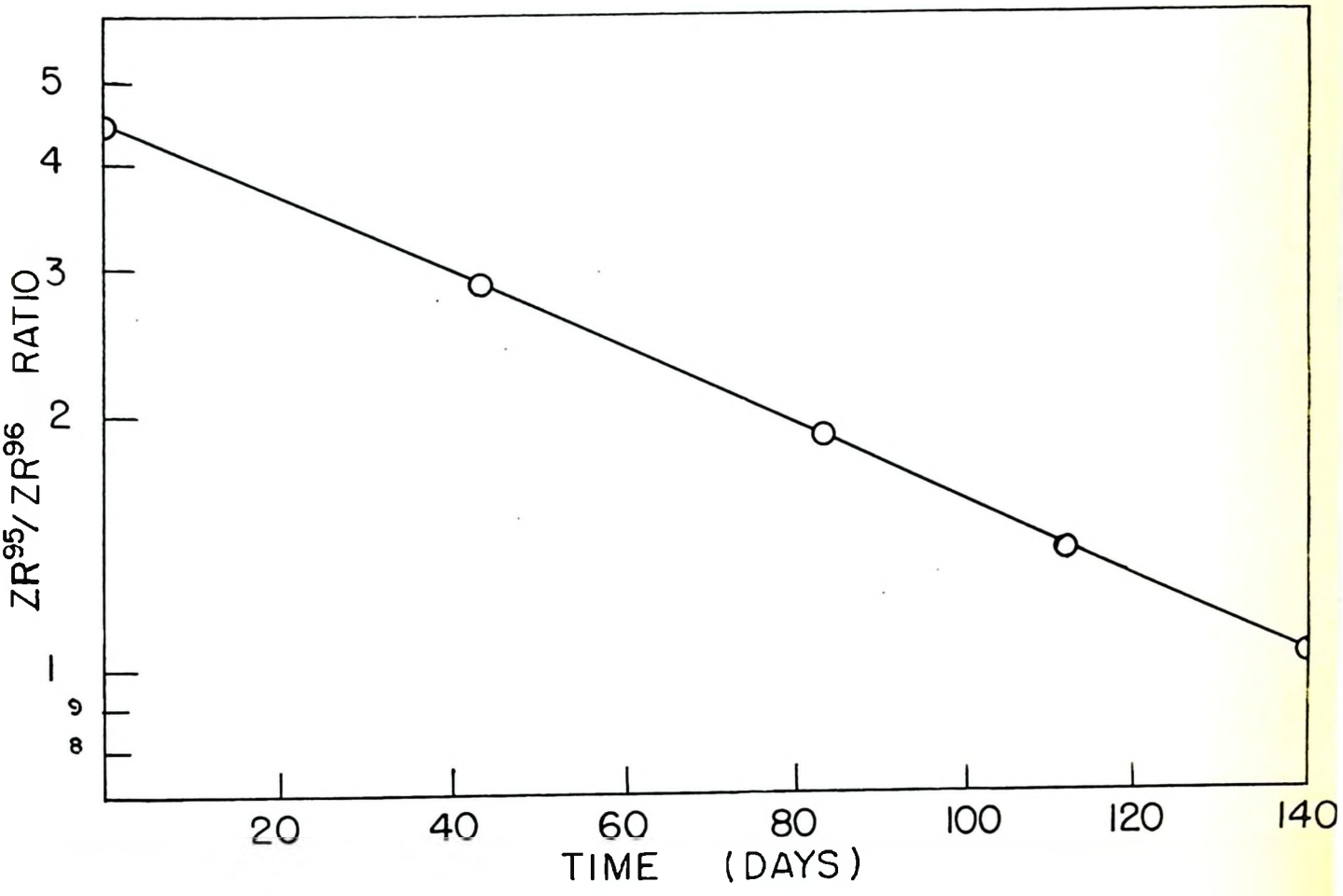

FIGURE 2 ZR^{95}/ZR^{96} VS TIME

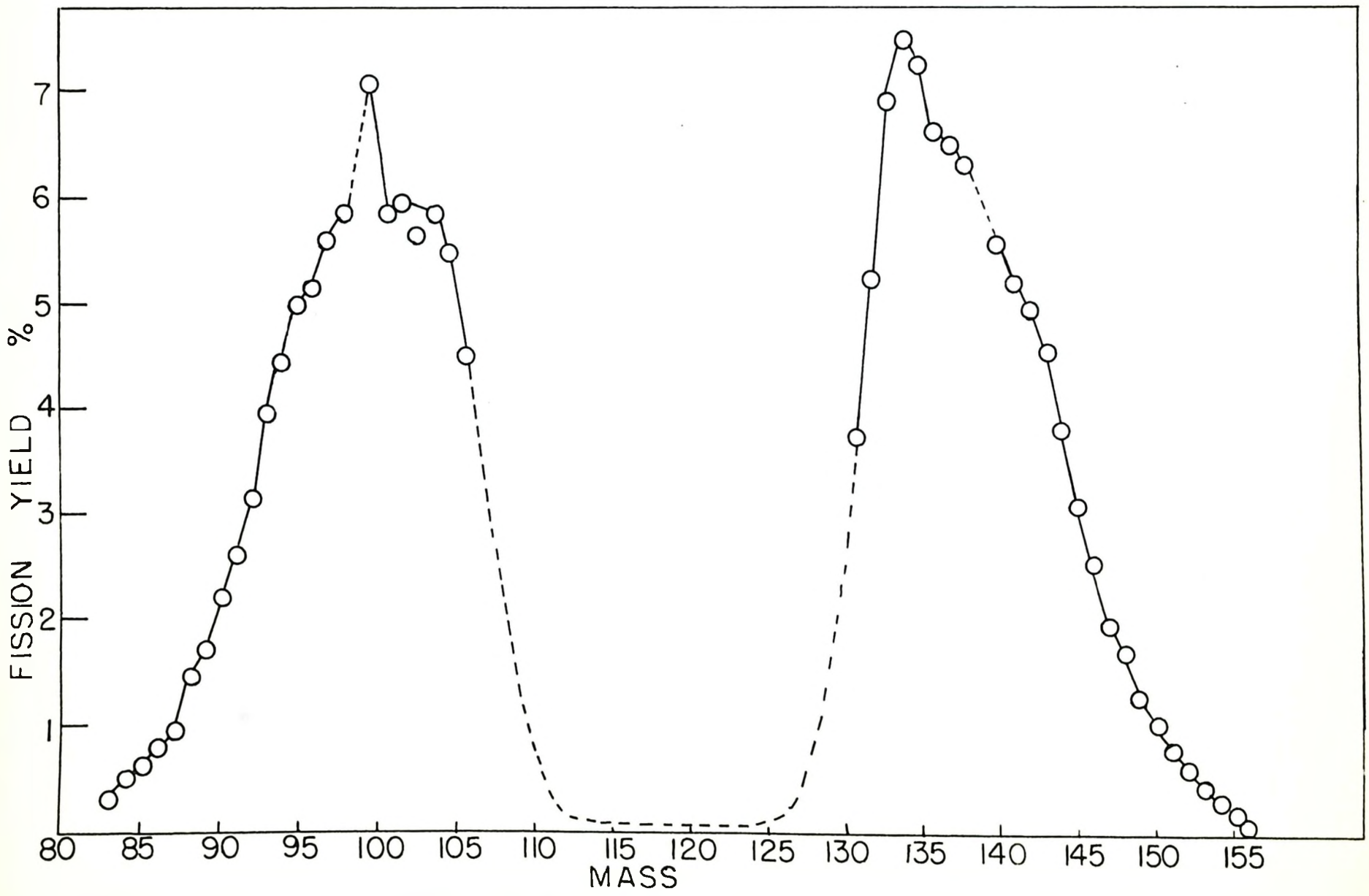

FIGURE 3 MASS YIELDS IN THERMAL NEUTRON FISSION OF PU^{239}

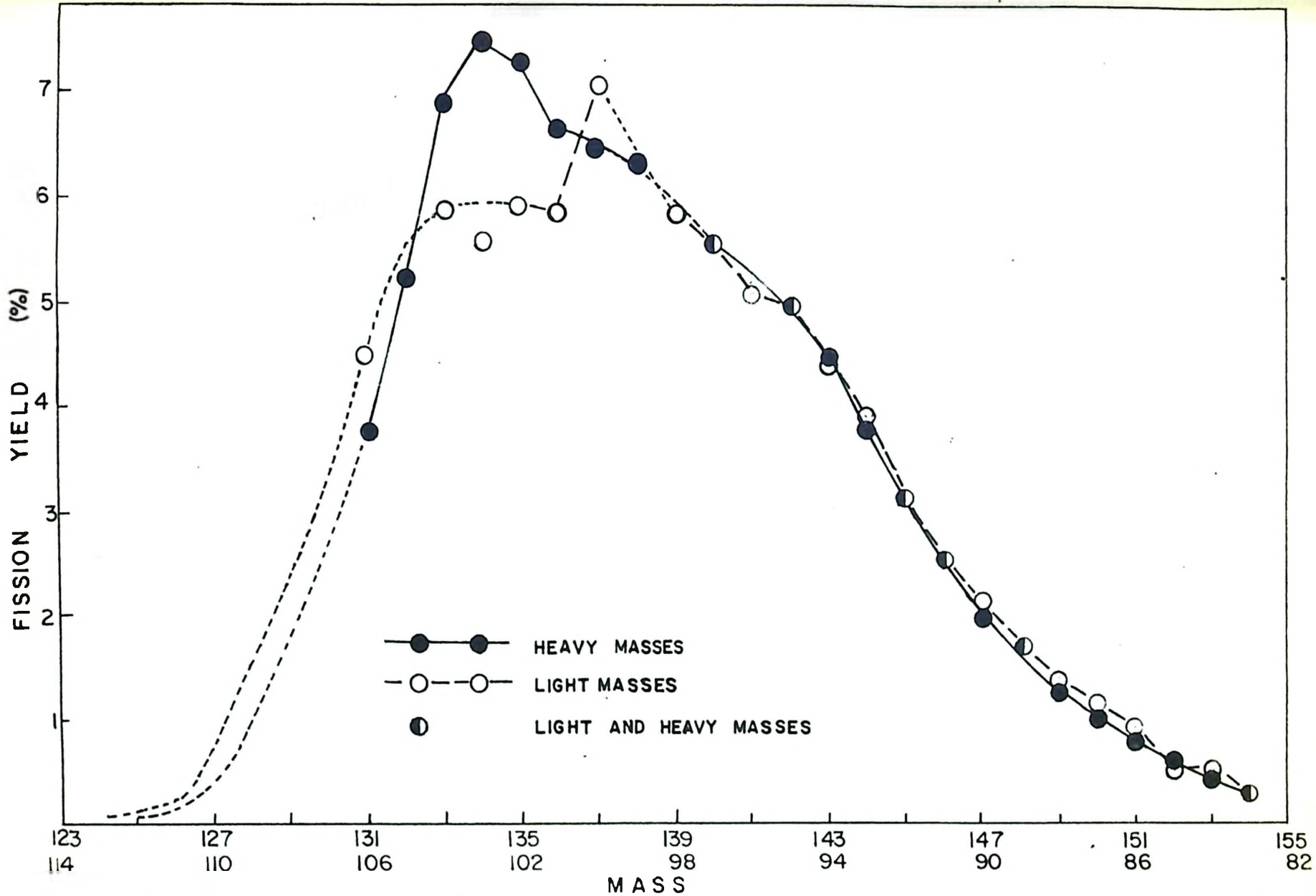

FIGURE 4 COMPARISON OF LIGHT AND HEAVY MASS YIELDS IN THERMAL NEUTRON FISSION OF PU^{239}

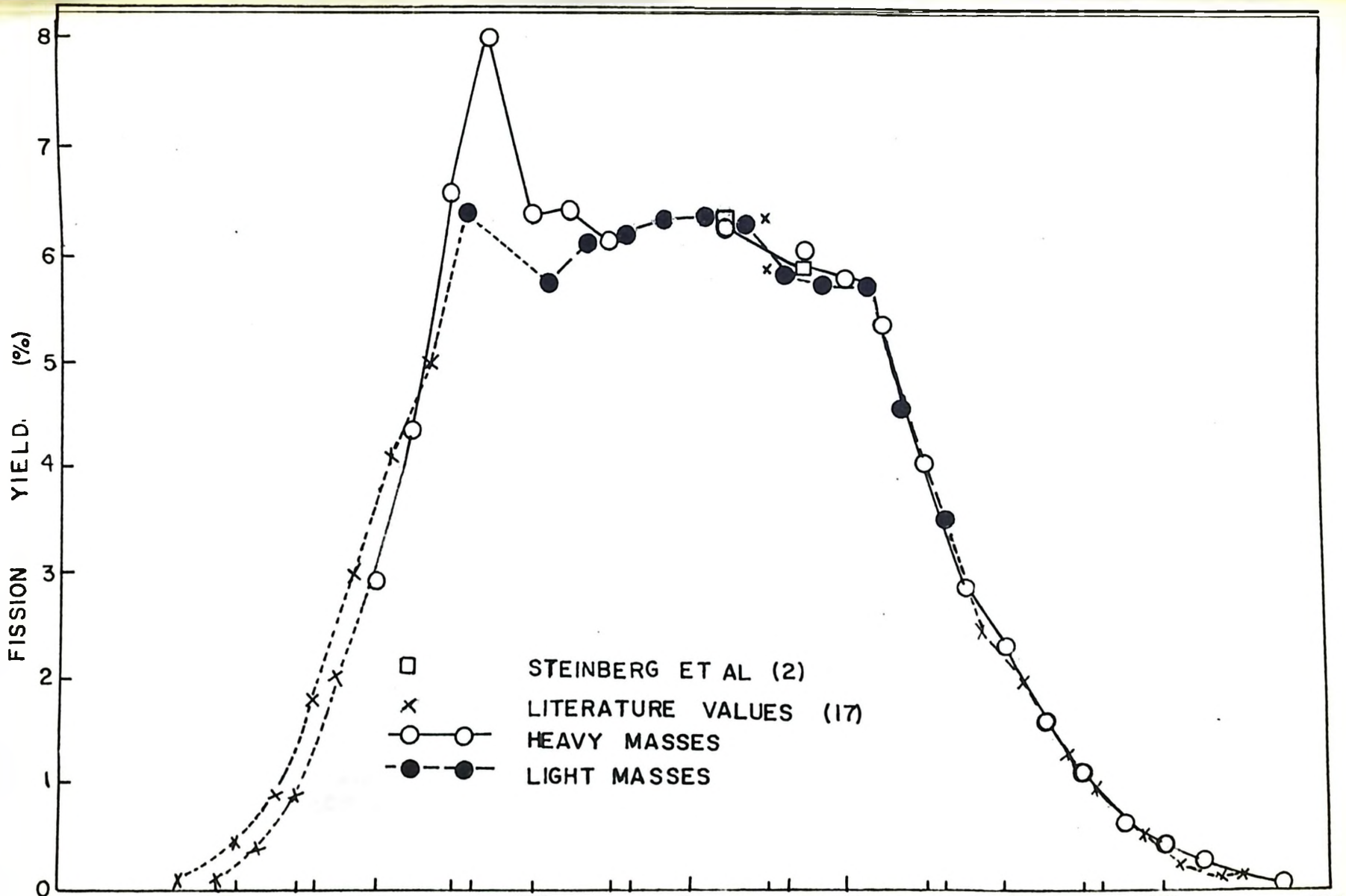

FIGURE 5 COMPARISON OF LIGHT AND HEAVY MASS YIELDS IN THERMAL NEUTRON FISSION OF U^{235}

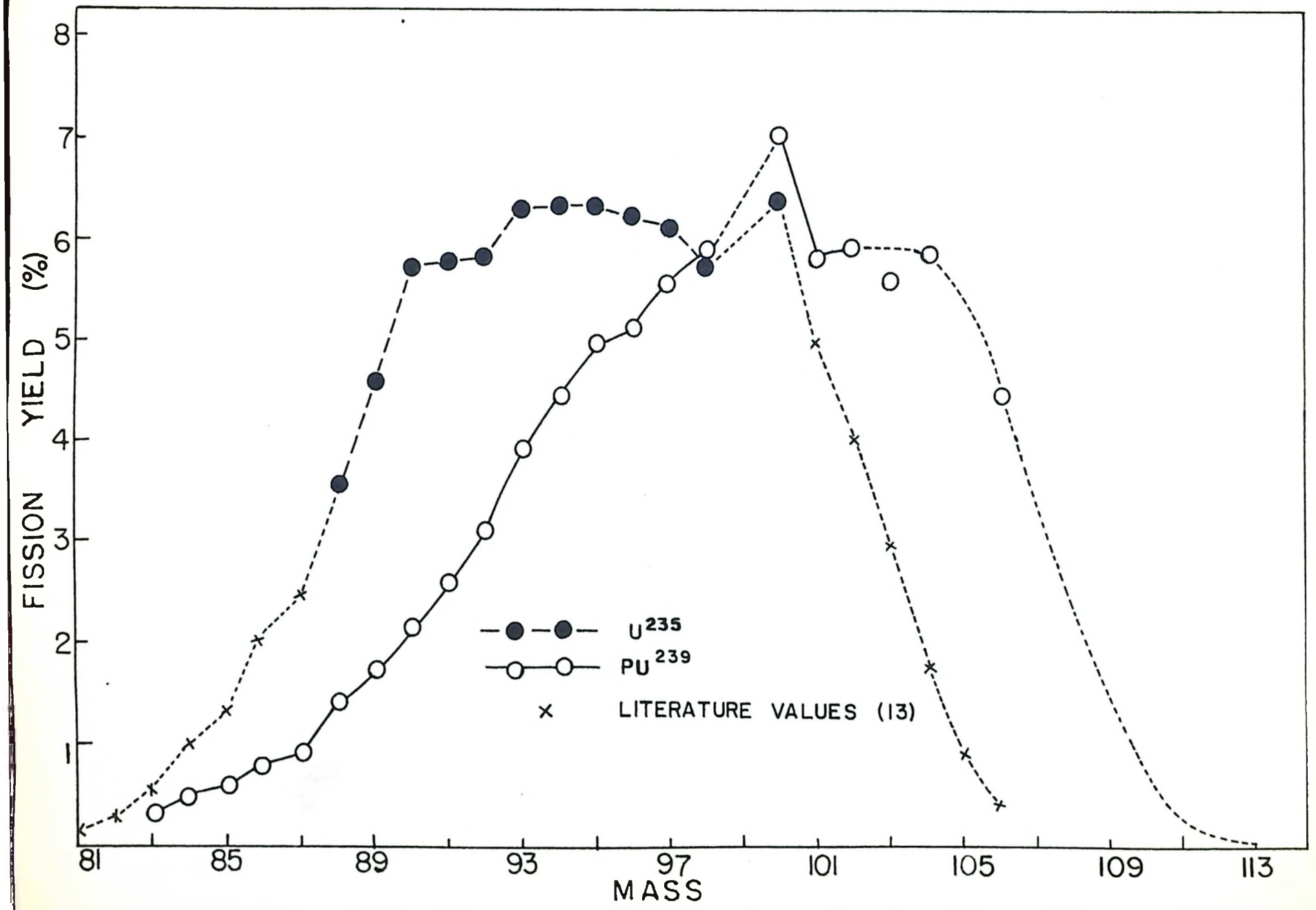

FIGURE 6 COMPARISON OF LIGHT MASS YIELDS IN THERMAL FISSION OF PU^{239} AND U^{235}

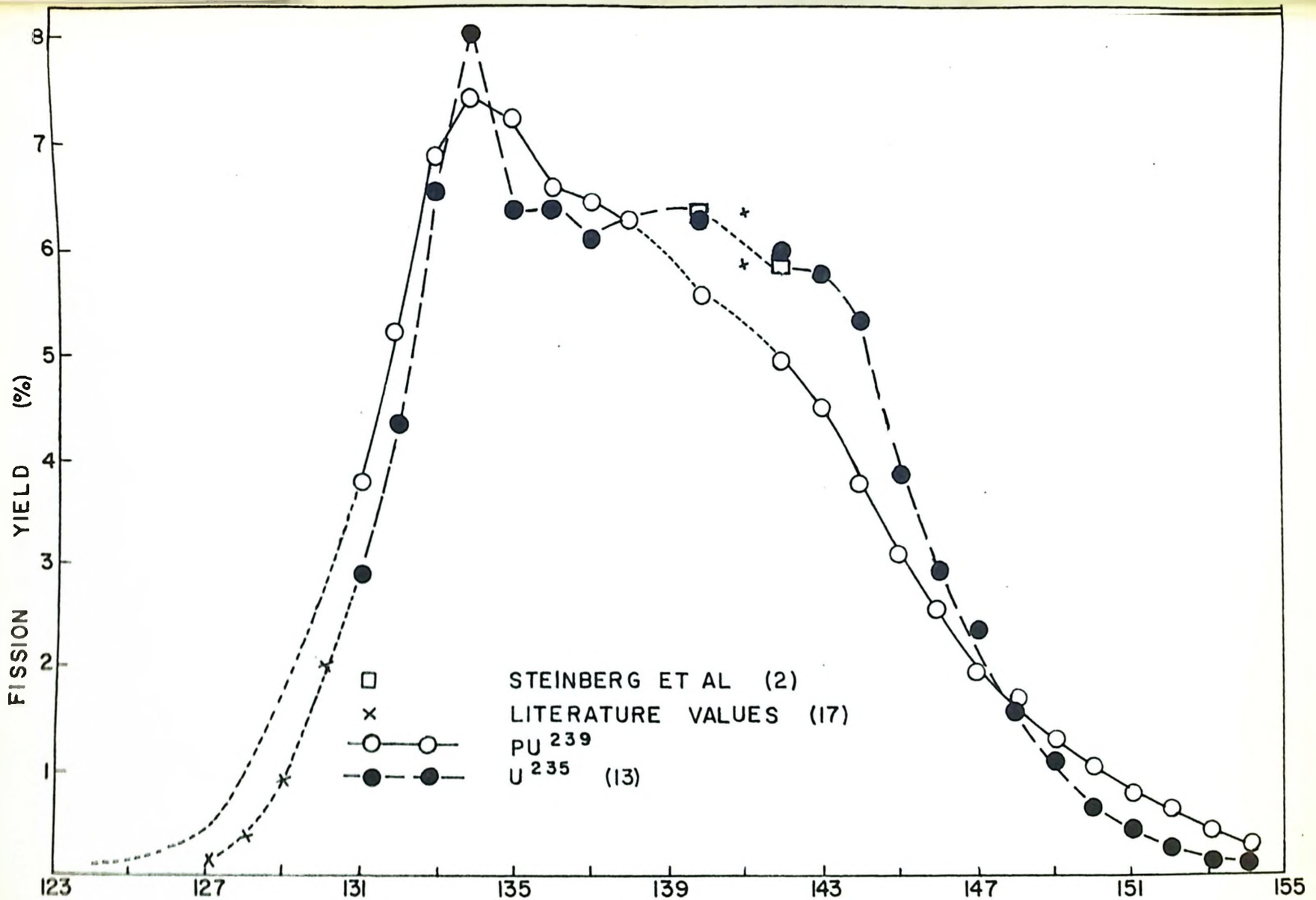

FIGURE 7 COMPARISON OF HEAVY MASS YIELDS IN THERMAL NEUTRON FISSION OF PU^{239} AND U^{235}